

## Accepted Manuscript

A novel bromodomain inhibitor, CPI-203, serves as an HIV-1 latency-reversing agent by activating positive transcription elongation factor b

Taizhen Liang, Xuanxuan Zhang, Fangyuan Lai, Jian Lin, Chenliang Zhou, Xinfeng Xu, Xinghua Tan, Shuwen Liu, Lin Li

PII: S0006-2952(19)30140-6  
DOI: <https://doi.org/10.1016/j.bcp.2019.04.005>  
Reference: BCP 13488

To appear in: *Biochemical Pharmacology*

Received Date: 29 January 2019

Accepted Date: 7 April 2019

Please cite this article as: T. Liang, X. Zhang, F. Lai, J. Lin, C. Zhou, X. Xu, X. Tan, S. Liu, L. Li, A novel bromodomain inhibitor, CPI-203, serves as an HIV-1 latency-reversing agent by activating positive transcription elongation factor b, *Biochemical Pharmacology* (2019), doi: <https://doi.org/10.1016/j.bcp.2019.04.005>

This is a PDF file of an unedited manuscript that has been accepted for publication. As a service to our customers we are providing this early version of the manuscript. The manuscript will undergo copyediting, typesetting, and review of the resulting proof before it is published in its final form. Please note that during the production process errors may be discovered which could affect the content, and all legal disclaimers that apply to the journal pertain.



**A novel bromodomain inhibitor, CPI-203, serves as an HIV-1 latency-reversing agent by activating positive transcription elongation factor b**

Taizhen Liang<sup>1, †</sup>, Xuanxuan Zhang<sup>1, †</sup>, Fangyuan Lai<sup>1</sup>, Jian Lin<sup>1, 2</sup>, Chenliang Zhou<sup>1</sup>, Xinfeng Xu<sup>1</sup>, Xinghua Tan<sup>3</sup>, Shuwen Liu<sup>1,\*</sup>, Lin Li<sup>1,\*</sup>

<sup>1</sup>*Guangdong Provincial Key Laboratory of New Drug Screening, Guangzhou Key Laboratory of Drug Research for Emerging Virus Prevention and Treatment, School of Pharmaceutical Sciences, Southern Medical University, Guangzhou, 510515, P. R. China;*

<sup>2</sup>*The Seventh Affiliated Hospital of Sun Yat-Sen University, Shenzhen, Guangdong 518107, P.R. China*

<sup>3</sup>*Department of Infectious Disease, Guangzhou No. 8 People's Hospital, Guangzhou, 510060, P. R. China.*

**\*Correspondence.** Shuwen Liu and Lin Li, School of Pharmaceutical Sciences, Southern Medical University, 1838 Guangzhou Avenue North, Guangzhou, Guangdong 510515, P. R. China. E-mail: [liusw@smu.edu.cn](mailto:liusw@smu.edu.cn); [li75lin@smu.edu.cn](mailto:li75lin@smu.edu.cn)

<sup>†</sup>Taizhen Liang and Xuanxuan Zhang share first authorship.

**Abstract**

The persistence of latent human immunodeficiency virus type 1 (HIV-1) reservoirs remains a major hurdle for HIV-1 eradication. The “shock and kill” strategy relies on the drug-mediated reversion of HIV-1 latency and the subsequent death of HIV-producing cells. Unfortunately, none of the agents currently in use possess a sufficient potency to reactivate latent virus or eliminate the latent HIV-1 reservoir *in vivo*. Here, we demonstrated that a promising specific bromodomain and extraterminal domain inhibitor, CPI-203, could potentially reactivate latent HIV-1 in different latently infected cell lines with minimal cytotoxicity by activating the positive transcription elongation factor b signaling pathway. Notably, CPI-203 exhibited synergism in latent HIV-1 reactivation and alleviated the HIV-1-induced “cytokine storm” when used in combination with the protein kinase C (PKC) agonist prostratin. These findings highlight that CPI-203 shows promise as a novel, safe candidate for the design of targeted strategies to “shock and kill” HIV-1 and thus represents a potential functional cure.

**Keywords:** latent HIV-1; shock and kill; latency-reversing agent; CPI-203; p-TEFb

## 1. Introduction

Combination antiretroviral therapy (cART) can potently suppress human immunodeficiency virus type 1 (HIV-1) viremia to undetectable levels and partially restore immune function in infected individuals. However, the interruption of cART clearly leads to a rapid rebound in plasma viremia to levels similar to those prior to therapy initiation [1], and the persistence of a latent HIV-1 reservoir is a major obstacle to eradicating infection. Latent proviruses in resting CD4<sup>+</sup> T cells express little HIV-1 RNA or protein, making them invisible to the immune response and antiviral drugs [2, 3]. In addition, resting CD4<sup>+</sup> T cells, peripheral blood monocytes, dendritic cells and macrophages are also involved in the establishment of a latently infected reservoir through the integration of HIV-1 [4]. Evidence is now accumulating that purging the HIV-1 reservoir might lead to a cure or remission [5, 6]. Therefore, therapeutic strategies to eliminate the HIV-1 latent reservoir are urgently needed.

One strategy, termed “shock and kill”, has recently gained substantial attention and has been developed as an HIV-1 functional cure [5, 7]. This therapeutic approach is based on the reactivation of dormant viruses from a latently infected HIV-1 reservoir followed by the eradication of the reservoir. Either HIV-1-specific cytolytic T lymphocytes (CTLs) or direct viral cytopathic effects after the reactivation of latent HIV-1 can presumably kill the latently infected cells.

Currently, some small-molecule HIV-1 latency-reversing agents (LRAs) have been developed to reactivate latent proviruses with the intent of purging latent HIV-1 [8, 9]. Early clinical trials investigating LRAs have demonstrated a significant increase in HIV-1 RNA production in the resting CD4<sup>+</sup> T cells of patients in whom viremia was fully suppressed by cART. However, some LRAs may be toxic or harmful to the host brain when administered for long periods or at high dosages. Moreover, HIV-associated exhaustion of the immune system hinders the efficient elimination of reactivated cells. Therefore, the identification of new, effective and safe LRAs that do not provoke broad T cell activation is essential and might be achievable by elucidating the host cell-mediated molecular mechanism and factors underlying viral latency.

The bromodomain (BRD) and extraterminal domain (BET) protein family comprise a well-conserved class of transcriptional regulators that are distinguished by the presence of tandem BRDs, conserved domains that recognize and bind acetyl-lysine residues. Targeting the binding of BET proteins to chromatin may provide an effective way to regulate HIV-1 gene expression and, in particular, transcription elongation [8, 10, 11]. The BET protein family in humans comprises four members (BRD2, BRD3, BRD4 and the testis-specific BRDT) [12]. The best-studied member, BRD4, containing a third functional domain, termed the positive transcription elongation factor b (p-TEFb)-interacting domain (PID), binds to the HIV-1 cofactor p-TEFb. The BRD4 inhibitor can interact with p-TEFb and favor the recruitment of p-TEFb by Tat to the HIV-1 promoter [13, 14]. A recent study showed that the short isoform of BRD4 (BRD4S) that lacks the PID can instead cooperate with SWI/SNF nucleosome remodelers to repress HIV-1 transcription during latency [15]. Therefore, BRD4 is a key regulator leading to the establishment of HIV-1 latency.

Notably, BET inhibitors (BETis) have been shown to reverse HIV-1 latency *in vitro* and *ex vivo* [10, 16, 17]. However, a reported BETi, JQ1, showed weak activity in reactivating latent viruses in latent HIV-1 models and exerted severe cytotoxicity during prolonged treatment. CPI-203 is a novel cell-permeable BETi with potent BRD4 selectivity and shows good bioavailability when administered orally [18-20]. Here, we demonstrated that CPI-203 effectively reactivated latent HIV-1 by increasing the cyclin-dependent kinase 9 (CDK9) occupancy and RNA Pol II carboxy terminal domain (CTD) phosphorylation levels in HIV-1 latency models *in vitro*. It is worth noting that CPI-203 could reverse HIV-1 latency with high efficacy when used in combination with prostratin. Importantly, CPI-203 exerted low toxicity and ameliorated the prostratin-induced “cytokine storm”, a severe, systemic production of inflammatory cytokines in response to endotoxemic shock. These results suggest that CPI-203-based BETis can potentially be further developed as new, safe LRAs to functionally cure HIV-1.

## 2. Materials and methods

### 2.1 Cell lines and culture

J-Lat A2 cells (harboring a 5'-LTR-Tat-Flag-iRES-EGFP-3'-LTR construct), J-Lat 10.6 cells (containing a full-length integrated HIV-1 genome with a defective envelope that expresses GFP upon activation), ACH2 cells (A3.01 chronically infected with HIV-1 with mutations in TAR), Jurkat cells (a parental cell line of J-Lat latency cell lines), A3.01 cells (HIV-1 uninfected parental cells) and THP-1 cells were cultured in RPMI 1640 medium (Gibco, Grand Island, NY, USA) supplemented with 10% fetal bovine serum (FBS, Gibco, Grand Island, NY, USA) and 1% penicillin/streptomycin (Invitrogen, Carlsbad, CA, USA) in a 37°C incubator containing 5% CO<sub>2</sub>.

### 2.2 Materials

CPI-203 was purchased from Selleck (Boston, MA, USA). Prostratin, phorbol 12-myristate 13-acetate (PMA) and lipopolysaccharide (LPS) were purchased from Sigma (St. Louis, MO, USA). JQ1 and SAHA were purchased from MedChemExpress (MCE, Vantaa, Finland). All chemicals were dissolved in anhydrous DMSO and stored at -20°C. Antibodies specific for BRD4, CDK9, Cyclin T1, Rpb1 CTD, p-Rpb1 and  $\beta$ -actin were purchased from Cell Signaling Technology (Beverly, MA, USA). Antibody specific to p-CDK9 (Thr186) were purchased from Santa Cruz Biotechnology (Santa Cruz, CA, USA). Antibody specific to p24 (183-12H-5C) was obtained from the National Institutes of Health AIDS Research and Reference Reagent Program. Human anti-CD25-FITC-, anti-CD69-FITC-, anti-HLA-DR-FITC-, and anti-CD38-FITC-conjugated antibodies and anti-CD4, anti-CCR5 and anti-CXCR4 antibodies were from BD Biosciences (San Jose, CA, USA). The J-Lat cell lines and ACH2 cells were kindly provided by Dr. Shibo Jiang and Dr. Lu (Fudan University, China).

Female C57BL/6J mice (7-8 weeks old, average weight, 20 to 25 g) were obtained from the Animal Research Centre of Southern Medical University. Animal experiments were performed in accordance with the animal protocol approved by the Institutional Animal Care and Use Committee (IACUC) as well as the Animal

Research Reporting *In Vivo* Experiments (ARRIVE) guidelines for animal research.

### **2.3 Flow cytometry**

J-Lat A2 and J-Lat 10.6 cells ( $5 \times 10^5$  cells) were incubated with the indicated concentrations of compounds for 48 h or the otherwise indicated amounts of time in 48-well plates. After washing three times with PBS, GFP expression was analyzed by a BD FACS Canto II flow cytometer (San Jose, CA, USA). The data were analyzed using FlowJo software (Treestar, San Carlos, CA, USA), and the percentage of GFP-positive cells within the entire population was used as a measure of HIV-1 reactivation.

### **2.4 HIV-1 antigen p24 assay**

ACH2 cells ( $5 \times 10^5$  cells) were seeded into 96-well plates and incubated with CPI-203 or JQ1 at different concentrations. Then, the cells were centrifuged, and the supernatants were collected and mixed with an equal volume of 5% Triton X-100. Viral release lysates were assayed for supernatant p24 antigen levels by ELISA as previously described [21].

### **2.5 Isolation of CD4<sup>+</sup> T cells from HIV-1-infected individuals**

HIV-1-infected patients were selected based on sustained plasma viral load suppression (plasma viral loads < 20 copies/ml for > 12 months and CD4 count > 350 cells/ml) and their essential information is listed in **Table 1**. Human peripheral blood mononuclear cells (PBMCs) were isolated by Ficoll density gradient centrifugation using Histopaque-1077 (Sigma-Aldrich). Primary CD4<sup>+</sup> T cells were isolated from PBMCs using an EasySep kit (STEMCELL Technologies Inc. Vancouver, BC, Canada) according to the manufacturer's instructions; a purity > 90% was achieved.

### **2.6 Real-time quantitative PCR (RT-qPCR)**

CD4<sup>+</sup> T cells isolated as described above were incubated with or without CPI-203 for 48 h, and intracellular HIV-1 RNA transcript expression was measured by RT-qPCR. The effects of CPI-203 on HIV-1 gene expression in ACH2 cells were also assessed by RT-qPCR. Briefly, total RNA was extracted using TRIzol (Invitrogen, Carlsbad, CA, USA), and cDNA was amplified using the PrimeScript RT Reagent Kit (TaKaRa, Japan). RT-qPCR was performed using SYBR Select Master Mix (TAKARA) on a

7500 Real-Time PCR system (Applied Bio-systems, Foster City, CA, USA) under the following conditions: 95°C for 15 s for initial denaturation, followed by 40 cycles of 95°C for 15 s and 60°C for 1 min for annealing and extension, respectively. The GAPDH gene served as the reference, and dimethyl sulfoxide (DMSO, Sigma, St. Louis, MO, USA) was used as the calibrator in all experiments. Relative gene expression levels were determined using the delta-delta CT ( $2^{-\Delta\Delta CT}$ ) method. The sequences of primers used for PCR amplification are listed in **Table 2**.

### **2.7 Cytotoxicity assay**

The *in vitro* cytotoxicities of CPI-203 on normal PBMCs from healthy individuals, Jurkat cells, J-Lat cells (A2 and 10.6), A3.01 cells and ACH2 cells were evaluated using the MTT (3-(4,5-dimethylthiazol-2-yl)-5-(3,4-diphenyltetrazolium) bromide, Sigma, St. Louis, MO, USA) assay as previously described [22]. Briefly, 100  $\mu$ l of CPI-203 at graded concentrations was added to equal volumes of cells ( $5 \times 10^5$  cells) in 96-well plates. After incubation at 37°C for 48 h, 20  $\mu$ l of the MTT solution (5 mg·ml<sup>-1</sup>) was added, and the plates were incubated for an additional 4 h. The cell-free supernatants were discarded, and formazan crystals were solubilized by DMSO. The colored formazan products were photometrically measured at 570 nm in a multiwell plate reader (Bio-Rad Laboratories, CA, USA). JQ1 was used as a control, and the 50% cytotoxicity concentration (CC<sub>50</sub>) was calculated using CalcuSyn software.

### **2.8 Detection of T cell activation markers and HIV-1 receptors/coreceptors**

PBMCs were isolated from the blood of healthy donors at Nanfang Hospital using standard density gradient centrifugation with Histopaque-1077 (Sigma, St. Louis, MO, USA), a protocol approved by the Human Ethics Committee of Southern Medical University in China.

To test the effects of CPI-203 on T cell activation,  $1 \times 10^6$  PBMCs were seeded in 6-well plates and incubated with CPI-203 for 24 or 72 h. After the incubation, the PBMCs were immunostained with anti-CD25-FITC-, anti-CD69-FITC-, anti-HLA-DR-FITC- and anti-CD38-FITC-conjugated antibodies (BD-Biosciences, San Jose, CA, USA) at 4°C for 20 min in the dark. Then, the cells were fixed in 1% paraformaldehyde (PFA, Sigma, St. Louis, MO, USA) and analyzed by BD



FACSCanto II flow cytometry. Prostratin was used as a positive control.

To evaluate the effects of CPI-203 on the expression of HIV-1 receptors/coreceptors,  $1 \times 10^6$  PBMCs were incubated with CPI-203 for 48 h. Cells were stained with anti-CD4/anti-CCR5 or anti-CD4/anti-CXCR4 antibodies (BD Bioscience, San Jose, CA, USA) at 4°C for 30 min in the dark and analyzed by flow cytometry.

### **2.9 Measurement of pro-inflammatory cytokine release by ELISA**

To measure the effects of CPI-203 on the release of pro-inflammatory cytokines, PBMCs ( $1 \times 10^6$  cells) were seeded in 96-well plates and incubated with CPI-203 or prostratin for 24 or 72 h. After the incubation, the supernatants were collected and subjected to ELISA according to the manufacturer's instructions (eBioscience, San Diego, CA, USA). The optical density (OD) was then recorded at a wavelength of 450 nm using a microplate reader (TECAN, Switzerland).

### **2.10 Western blot (WB) analysis**

WB analysis was performed as described previously [23]. Briefly, ACH2 cells were treated with CPI-203 at different concentrations or various amounts of time. After washing the cultured cells with PBS 2 times, the cells were lysed by RIPA buffer containing protease and phosphatase inhibitors (Merck, NY) on ice for 15 min and were then centrifuged at 12,000 g for 15 min at 4°C. The supernatants were collected in a fresh tube, and approximately 50 to 150 µg of the thermally denatured protein extract was separated on a 10% polyacrylamide gel, electroblotted onto a PVDF membrane (Roche, Indianapolis, IN, USA), and blocked for 1 h. The membrane was then incubated with antibody. Subsequently, enhanced chemiluminescence (ECL) substrates (Cell Signaling Technology) were added, and the blots were exposed to film to develop the image.

### **2.11 Coimmunoprecipitation (co-IP)**

ACH2 cells were treated with CPI-203 (1 µM) or JQ1 (1 µM) for 48 h. After washing the cultured cells with cold PBS 2 times, the protein extracts were harvested by the addition of cold IP lysis buffer (50 mM Tris (pH 8.0), 150 mM NaCl, 2 mM EDTA and 1% NP-40). Briefly, precleared protein extracts were added to the protein A/G

agarose (Santa Cruz, CA, USA) that was incubated with 1  $\mu$ g of an anti-BRD4 antibody (CST) on a rotator overnight. The lysate-agarose/antibody conjugate mixture was incubated overnight at 4°C on a rocking platform. The input control contained 10% of protein. After centrifuging at 2,500 rpm for 5 min, the pellet was washed with cold IP lysis buffer containing 0.1% phenylmethane sulfonyl fluoride (PMSF) five times. Subsequently, the precipitation was resuspended in loading buffer and subjected to WB analysis with the indicated antibodies.

### **2.12 Chromatin immunoprecipitation (ChIP)**

Chromatin immunoprecipitation (ChIP) assays were performed using a ChIP assay kit (Cell Signaling Technology, Beverly, MA, USA) according to the manufacturer's protocol and previously described procedures [24]. Briefly, ACH2 cells ( $1 \times 10^7$  cells) were treated with CPI-203 or JQ1 for 48 h and fixed with 1% formaldehyde for 10 min at room temperature, and crosslinking was quenched by the addition of glycine solution. The cross-linked cells were resuspended by lysis buffer and sonicated to obtain DNA fragments of 150 to 1000 bp. DNA fragments were incubated with IgG, CDK9 and Pol II CTD-Ser2P (CST) antibodies at 4°C overnight, and immune complexes were retrieved by incubating with protein A/G beads. Following washing, the chromatin was eluted from the protein A/G magnetic beads. DNA was extracted, and quantitative real-time PCR was performed using the SYBR-Green Mix on a Roche LightCycler 480 machine with forward (5'-AGCTTGCTACAAGGGACTTTCC-3') and reverse (5'-GTGGGTTCCTAGTTAGCCAGAG-3') primers. The results from fragments obtained after incubation with different antibodies were normalized against input DNA and are presented as the fold change relative to the DMSO control.

### **2.13 Synergistic reactivation of latent HIV-1 expression by CPI-203 and LRAs**

The reactivation of latent HIV-1 expression by CPI-203 alone, a histone deacetylation inhibitor (HDACi, SAHA) alone, prostratin alone, and the combination of CPI-203 with each of these LRAs in latently infected HIV-1 cell lines was assessed as previously described [24]. The percentage of GFP-positive cells within the entire population or the HIV-1 p24 antigen was used as a measure of HIV-1 reactivation.

The data were analyzed for the combined effects of multiple drug applications using the Bliss independence model as previously described [25]. For drugs  $x$  and  $y$ , the equation  $f_{axy,p} = f_{ax}$  (the observed effects of drug  $x$ ) +  $f_{ay}$  (the observed effects of drug  $y$ ) -  $(f_{ax})(f_{ay})$  was used. For calculating  $f_{ax}$  of the ACH2 cells, the approach is defined as based on a protocol as Larid:  $f_{ax} = (\text{HIV p24 levels of drug } x - \text{HIV p24 levels of DMSO mock}) / (\text{HIV p24 levels of PMA} - \text{HIV p24 levels of DMSO mock})$ . Correspondingly, the calculation of  $f_{ax}$  for J-Lat cells used the %GFP-positive cells in place of HIV p24 levels. Based on this model,  $\Delta f_{axy} = f_{axy,o}$  (the experimentally observed fraction affected by the drug combination) -  $f_{axy,p}$  (the predicted fraction affected by a combination of drug  $x$  and drug  $y$ ). Here,  $\Delta f_{axy}$  provides an indication of the synergy ( $\Delta f_{axy} > 0$ ), additive effect (Bliss independence) ( $\Delta f_{axy} = 0$ ) or antagonism ( $\Delta f_{axy} < 0$ ).

#### **2.14 Anti-inflammatory effects of CPI-203 in vitro and in vivo**

THP-1 cells ( $5 \times 10^5$  cells) were seeded and differentiated with  $10 \text{ ng}\cdot\text{ml}^{-1}$  phorbol 12-myristate 13-acetate (PMA, Sigma, St. Louis, MO, USA) for 24 h. After incubation with CPI-203, prostratin or lipopolysaccharide (LPS, *E. coli* serotype 0111:B4 endotoxin; Sigma, St. Louis, MO, USA) was added for 12 h, after which the supernatants were collected and subjected to ELISA according to the manufacturer's instructions (eBioscience, San Diego, CA, USA). Cells were also collected for RNA extraction and measurement of pro-inflammatory cytokine expression by RT-qPCR as described above. JQ1 was chosen as a positive control.

To test the anti-inflammatory effects of CPI-203 on LPS-stimulated mice, female C57BL/6J mice were randomly assigned into 4 groups ( $n = 6$  per group): control (treated with physiological saline); LPS ( $15 \text{ mg}\cdot\text{kg}^{-1}$ ); CPI-203 ( $50 \text{ mg}\cdot\text{kg}^{-1}$ ); and CPI-203 + LPS. First, mice of the CPI-203 group were administered CPI-203 ( $50 \text{ mg}\cdot\text{kg}^{-1}$ ) daily via intraperitoneal (i.p.) injection for 5 days. Correspondingly, mice of the control and LPS groups were injected with physiological saline. After 5 days, mice of both the LPS and CPI-203 + LPS groups were administered LPS ( $15 \text{ mg}\cdot\text{kg}^{-1}$ ) i.p. to induce lung injury. After 8 h of LPS administration, all animals were sacrificed, and their lung tissues and sera were collected for further analysis. The tissues were

first fixed in 10% neutral buffered formalin, and the paraffin sections (5  $\mu\text{m}$ ) were then stained with hematoxylin and eosin (H&E). Serum samples were harvested and centrifuged for 10 min at 4,000 r/min. Then, the supernatant was stored at  $-80^{\circ}\text{C}$  before being subjected to ELISA according to the manufacturer's instructions.

### **2.15 Immunohistochemical analysis**

Lung tissues were fixed in 10% formalin overnight, paraffin-embedded, cut into 5- $\mu\text{m}$ -thick sections and placed on 3-aminopropyltriethoxysilane-coated slides. Then, the sections were deparaffinized with xylene, rehydrated with ethanol, and subjected to antigen retrieval using a microwave. Endogenous peroxidase activity was suppressed by incubating the samples with 1% hydrogen peroxide for 30 min. The sections were incubated with a mouse monoclonal ICAM1 antibody (1:100, Abcam, Cambridge, UK) at  $4^{\circ}\text{C}$  overnight. After washing three times, the sections were successively incubated with the appropriate horseradish peroxidase (HRP)-conjugated secondary antibodies and the detection substrates before being counterstained with hematoxylin.

### **2.16 Ethics statement**

The patients' peripheral blood was collected from HIV-1-infected patients at the Eighth People's Hospital of Guangzhou (Guangzhou, China) after informed consent was obtained. The experiment was approved by the Ethics Committee of The Eighth People's Hospital of Guangzhou (Approval Number is 20170380) and was performed in accordance with relevant guidelines and regulations.

### **2.17 Statistical analysis**

Experimental data are presented as the mean  $\pm$  SD of at least three independent experiments. The experimental procedures or treatment and data analyses were performed with randomization and blinding. Statistical analysis was calculated with GraphPad Prism 5.0 (GraphPad Software, San Diego, CA, USA). One-way ANOVA followed by Dennett's multiple comparison *post hoc* test was used to detect differences between the groups.  $p < 0.05$  was considered significant:  $p$  values were defined as  $*p < 0.05$ ,  $**p < 0.01$ ,  $^{\#}p < 0.05$  and  $^{\#\#}p < 0.01$ .

### 3. Results

#### *3.1 CPI-203 activates HIV-1 expression in latently infected cell lines in a dose- and time-dependent manner*

To confirm the potential activation of CPI-203 on latent HIV-1 expression, we investigated the effects of CPI-203 on well-established latently infected Jurkat T cell lines, including J-Lat A2 and 10.6 cells. J-Lat A2 cells contain a single provirus integrated into the intron of RNPS1 and an EGFP gene under the control of the HIV-1 long terminal repeat (LTR) [24]. J-Lat 10.6 cells contain a full-length integrated HIV-1 genome with HIV-1  $\Delta$ env from the NL4-3 backbone and a GFP reporter gene in place of the *Nef* gene [26]. The percentages of GFP-positive cells in these two cell lines after treatment with CPI-203 at different concentrations were analyzed by flow cytometry. The magnitude of reactivation induced by 10 ng/ml of PMA was defined as 100% reactivation, and an obvious dose-dependent increase in the percentage of GFP-positive cells treated with CPI-203 was observed compared to the background levels (**Fig. 1A, C**). As shown in **Fig. 1A**, when the CPI-203 concentration increased from 0.01  $\mu$ M to 25  $\mu$ M, the percentage of GFP-positive cells increased from 32.47% to 61.98%. Notably, CPI-203 was shown to induce HIV-1 reactivation more potently than JQ1, which is known as a BETi to reactivate HIV-1 from latency. Correspondingly, when the JQ1 concentration increased from 0.01  $\mu$ M to 5  $\mu$ M, the percentage of GFP-positive cells increased from 30.86% to 50.37%. It is worth noting that the percentage of GFP-positive cells gradually decreased when the JQ1 concentration exceeded 5  $\mu$ M due to cytotoxicity.

The kinetics of HIV-1 reactivation induced by CPI-203 were further measured in J-Lat A2 (**Fig. 1B**) and 10.6 (**Fig. 1D**) cells. The percentages of GFP-positive J-Lat A2 and 10.6 cells treated with 1  $\mu$ M CPI-203 increased as a function of time and reached approximately 45.10% and 27.93% at 72 h, respectively, while the percentages of GFP-positive J-Lat A2 and 10.6 cells treated with 1  $\mu$ M JQ1 for 72 h were only 34.15% (**Fig. 1B**) and 22.40% (**Fig. 1D**), respectively.

The reactivation effect of CPI-203 was further confirmed in ACH2 cells

chronically infected with latent HIV-1, which were derived from A3.01 [27, 28]. The production of the HIV-1 p24 antigen in the supernatants of cells cultured in the presence of CPI-203 was detected by ELISA. Consistently, CPI-203 promoted HIV-1 p24 expression in ACH2 cells in a dose- and time-dependent manner (**Fig. 1E, F**). As shown in **Fig. 1E**, the production levels of HIV-1 p24 in the supernatants of cells were obviously increased when the concentrations of CPI-203 ranged from 0.01  $\mu\text{M}$  to 50  $\mu\text{M}$ . However, the HIV-1 p24 levels were gradually decreased when the concentration of CPI-203 was increased to 100  $\mu\text{M}$ . A potential reason for this effect is that strong reactivation and active viral production may cause a strong CPE (cytopathic effect) and the rapid death of ACH2.

### ***3.2 CPI-203 activates HIV-1 transcription from latency in CD4<sup>+</sup> T cells from cART-treated individuals***

The data generated in HIV-1-infected cell lines may not be directly relevant to patients because of phenotypic differences. To address whether CPI-203 can effectively induce latent HIV-1 expression in CD4<sup>+</sup> T cells *ex vivo*, we further analyzed the effects of CPI-203 on HIV 5'-LTR transcription in CD4<sup>+</sup> T cells isolated from cART-treated HIV-infected individuals using RT-qPCR. As shown in **Fig. 2A**, an increase in full-length HIV-1 transcripts was observed in all six donors after treatment with CPI-203 (1  $\mu\text{M}$ ), and all transcripts showed > 2-fold induction. Here, JQ1 (2  $\mu\text{M}$ ) induced an increase in five of six donors, with five showing > 2-fold induction. SAHA and prostratin at 1  $\mu\text{M}$  induced increases in all six donors, but only three and five donors showed inductions > 2-fold (**Fig. 2A**).

### ***3.3 CPI-203 stimulates the transcription of HIV-1 genes***

The transcription levels of HIV-1 genes, including *Gag*, *Tat*, *Vpr*, *Vif* and *LTR*, were quantitatively analyzed by RT-qPCR. As shown in **Fig. 2B**, CPI-203 efficiently stimulated the transcription of all tested HIV-1 genes in a dose-dependent manner, indicating that CPI-203 is highly potent at inducing HIV-1 reactivation and latent HIV-1 transcription.

### ***3.4 CPI-203 displays minimal toxicity***

The efficacy of an LRA depends on the balance between its highly potent reactivity

and safety during clinical use. Therefore, we evaluated the cytotoxicity of CPI-203 on latently infected HIV-1 cell lines, including J-Lat A2, J-Lat 10.6, ACH2, Jurkat and A3.01 cells, as well as human PBMCs. CPI-203 induced minimal levels of cellular toxicity on all tested cells, as determined using the MTT assay, with  $CC_{50}$  values ranging from 124.94 to 358.17  $\mu\text{M}$ . The  $CC_{50}$  values of CPI-203 were more than 100 times higher than the effective dosage (1  $\mu\text{M}$ ) required to induce HIV-1 reactivation, and the  $CC_{50}$ s of CPI-203 toward two parental cells were higher than those for HIV-1 latent cells, indicating that CPI-203 could kill latently infected HIV-1 cells more specifically than HIV-1-noninfected cells (**Table 3**). Notably, the  $CC_{50}$  values of JQ1 on the tested cells ranged from 22.79 to 43.42  $\mu\text{M}$ . Furthermore, the log P values of CPI-203 and JQ1 were calculated using Chemdraw software. As shown in **Table 3**, the log P value for CPI-203 was 4.06 and that for JQ1 was 5.85, indicating that the absorption of CPI-203 is better than that of JQ1.

In addition, we also used the Toxicity Estimation Software Tool (TEST) to estimate the toxicity of CPI-203 and JQ1 according to Quantitative Structure Activity Relationships (QSARs) methodologies from the United States Environmental Protection Agency. The results showed that, in a rat model, CPI-203 was relatively safe, with 50% lethal doses ranging from 2280.31 to 3337.72  $\text{mg}\cdot\text{kg}^{-1}$ , substantially safer than JQ1 (243.27 to 2605.88  $\text{mg}\cdot\text{kg}^{-1}$ ) (**Table 3**). Taken together, all of the results indicated that CPI-203 is safer than JQ1 and, hence, has improved clinical utility.

### ***3.5 CPI-203 does not induce global T cell activation or inflammatory cytokine release***

One of the disadvantages of current LARs is their propensity to nonspecifically activate bystander T cells, which potentially releases pro-inflammatory cytokines, thus resulting in undesirable cell toxicity [25]. Ideally, LRAs should be able to penetrate anatomical sanctuaries and immune cell types without inducing global T cell activation [29-31]. To address this problem, we evaluated the effects of CPI-203 on the expression of T cell activation biomarkers by flow cytometry. Treatment with CPI-203 for 24 h or 72 h did not significantly alter the expression of CD69, CD38,

CD25 or HLA-DR in human PBMCs (**Fig. 3A, B**). Furthermore, no significant increases in the expression levels of the cytokines analyzed (TNF- $\alpha$ , IFN- $\gamma$ , IL-2 and IL-6) were observed in PBMCs harvested from healthy HIV-negative donors after treatment with CPI-203 for 24 or 72 h (**Fig. 3C**). Consistent with previously published studies [31], the positive control prostratin dramatically increased the expression levels of T cell activation biomarkers, especially CD69, CD25 and HLA-DR, and significantly upregulated the release of pro-inflammatory cytokines following stimulation for 24 or/and 72 h (**Fig. 3A-C**).

### ***3.6 CPI-203 downregulates the expression of HIV-1 receptors/coreceptors***

The first step of HIV-1 entry is the binding of the HIV-1 envelope protein to the cellular CD4 receptor. The second step is mediated by HIV-1 chemokine coreceptors, including the CXCR4 and CCR5 coreceptors expressed on the surface of CD4<sup>+</sup> T lymphocytes [32]. Thus, we further investigated the effects of CPI-203 on the expression of HIV-1 receptors and coreceptors. Our data showed that stimulation by CPI-203 markedly reduced the cell surface expression levels of CXCR4, CCR5 and CD4 (**Fig. 3D, E**). The capacity of CPI-203 to downregulate the expression of HIV-1 receptors/coreceptors might be beneficial for blocking viral spread to uninfected bystander CD4<sup>+</sup> T cells during the reactivation of HIV-1 latency, making it an attractive potential candidate for clinical studies investigating cures for HIV-1.

### ***3.7 CPI-203 promotes HIV-1 transcription via the p-TEFb pathway***

As it is well known that JQ1 activates the p-TEFb pathway, we wanted to determine whether CPI-203 can influence p-TEFb in latent cells. Surprisingly, no significant changes in the expression levels of CDK9 or Cyclin T1 were observed after treatment with CPI-203 at different concentrations or for different amounts of time (**Fig. 4A-D**). However, the phosphorylation of CDK9 at Thr186, which is located at the tip of the CDK9 T-loop and is required for the catalytic activity of CDK9 [33, 34], was upregulated in both a dose- and time-dependent manner, consistent with the expression levels of the HIV-1 capsid protein p24 (**Fig. 4**). CDK9 is well known to promote HIV-1 gene transcription elongation by phosphorylating Pol II at serine 2 (Ser2) [35]. To further identify whether CPI-203 affects the phosphorylation of the



RNA Pol II CTD, the proteins Rpb1 and phospho-Rpb1 CTD on Ser (CTD-Ser2P) were analyzed by WB. As shown in **Fig. 4**, p-Rpb1 CTD-Ser2P was also significantly increased by CPI-203 in both a dose- and time-dependent manner, indicating that CPI-203 activates latent HIV-1 by increasing CDK9 phosphorylation and inducing RNA Pol II CTD phosphorylation.

The HIV-1 promoter-bound BRD4-p-TEFb immune complex has been shown to competitively block the interaction of Tat with p-TEFb (by interacting with acetylated histones, or Ac) [17, 35], leading to abortive transcriptional elongation. Therefore, a coimmunoprecipitation experiment was performed to elucidate the effects of CPI-203 on the interaction between BRD4 and p-TEFb. As shown in **Fig. 5A**, the p-TEFb subunits CDK9 and CyclinT1 were released by BRD4 in ACH2 cells after treatment with CPI-203 for 48 h. Next, we also sought to determine whether CPI-203 affected the occupancy of p-TEFb and the phosphorylation of RNA Pol II CTD at the HIV-1 promoter. To this end, ChIP-qPCR assays were performed with ACH2 cells treated with 1  $\mu$ M CPI-203 or JQ1. As expected, CPI-203 treatment resulted in BRD4 dissociation from the HIV-1 LTR promoter and caused a 3.3-fold increase in the level of CDK9 bound to the HIV-1 promoter compared with the control. This increase, in turn, resulted in enhanced phospho-Rpb1 CTD on Ser (CTD-Ser2P) (3.2-fold increase over the control) (**Fig. 5B**). Together, these results indicated that CPI-203 can significantly dissociate BRD4 from the HIV-1 promoter, allowing Tat to bind to p-TEFb and assemble a functional SEC on the TAR stem-loop structure for phosphorylation of the Pol II CTD, thus activating HIV-1 transcription.

### **3.8 CPI-203 synergistically reactivates latent HIV-1**

Several cell signaling pathways are critical for the establishment and maintenance of HIV-1 latency, and LRAs with a single mechanism may not be sufficient to reverse latency. Combinational LRA strategies are widely assumed to more efficiently reactivate the latent HIV-1 reservoir than single LRAs. Here, J-Lat A2 and ACH2 cells were first treated with CPI-203 (0.1  $\mu$ M), prostratin (0.5  $\mu$ M), SAHA (0.5  $\mu$ M) or their combinations for 48 h, with PMA stimulation serving as the positive control. As shown in **Fig. 6A, B**, treatment with LRA (CPI-203, prostratin and SAHA) alone

did not increase GFP<sup>+</sup> cells and supernatant p24 levels. However, once prostratin or SAHA were combined with CPI-203, they markedly enhanced the effect (**Fig. 6A, B**). A similar result was also observed in primary CD4<sup>+</sup> T cells from HIV-infected patients *ex vivo* (**Fig. 6E**). Based on the Bliss independence model, the combined effects of CPI-203 with prostratin and SAHA were greater than the idealized Bliss independence prediction ( $\Delta f_{axy} > 0$  defined as synergism) (**Fig. 6C, D**). Thus, the combination of CPI-203 with conventional chemical latency activators, such as prostratin and SAHA, might be an effective way to reverse HIV-1 latency.

### ***3.9 CPI-203 inhibits LPS- or prostratin-stimulated inflammatory cytokine expression***

As previously reported, the PKC agonist prostratin can nonspecifically induce global T cell activation and potential cytokine release by regulating the NF- $\kappa$ B pathway. It has been reported that JQ1 can inhibit inflammatory cytokine release by disrupting the interaction between BET proteins and targets in LPS-stimulated macrophages and LPS-induced endotoxemic shock mice [36-38]. As the aforementioned observations showed that CPI-203 and prostratin had strong synergistic activation (**Fig. 6**), we investigated whether CPI-203 could also reduce the side effects of prostratin by inhibiting inflammatory cytokine release. As shown in **Fig. 7A and 7C**, CPI-203 significantly decreased the prostratin-mediated production of inflammatory cytokines (IL-1 $\beta$ , IL-6, TNF- $\alpha$  and MCP-1) in THP-1 cells. Similar results further confirmed that CPI-203 significantly decreased the release of inflammatory cytokines in LPS-stimulated THP-1 cells (**Fig. 7B, D**). Furthermore, CPI-203 significantly reduced the levels of secreted inflammatory cytokines (IL-1 $\beta$ , IL-2, IL-6 and TNF- $\alpha$ ) in the sera of LPS-challenged mice (**Fig. 8A**). The H&E-stained lungs of LPS-challenged mice showed increased thickness of the alveolar wall and significant inflammatory cell infiltration (**Fig. 8B**). However, the pathological changes observed in the lungs of LPS-challenged mice treated with CPI-203 were weaker than those observed in the lungs of the LPS-treated mice. In addition, CPI-203 obviously decreased the expression of ICAM-1 in the lungs of LPS-challenged mice compared with those of LPS control group mice (**Fig. 8B**). Collectively, our data indicate that CPI-203 and

prostratin could be a promising combination that has a high synergistic activation and the capacity to suppress inflammatory cytokine production.

#### 4. Discussion

Despite the complete suppression of detectable viremia by cART, viremia rapidly rebounds after treatment interruption due to the existence of a latent viral reservoir. The “shock and kill” strategy designed to eradicate latent HIV-1 relies on the discovery of novel LRAs that can reactivate the latent HIV-1 reservoir without significantly impacting the growth and function of host cells [39]. Unfortunately, the currently available LRA candidates have shown high toxicity and/or poor clinical outcomes.

Data from this study showed that the BETi CPI-203 can potently reactivate latent HIV-1 expression in both latently infected cell models and resting CD4<sup>+</sup> T cells obtained from HIV-1-infected individuals undergoing suppressive cART. Previous studies have reported that the BETi JQ1 can reactivate HIV-1 from latency [16, 17]. Although CPI-203 shares a similar core structure with JQ1, the ester chain of JQ1 is replaced with an amino side chain in CPI-203, and these structural differences may alter the physicochemical properties, biological functions and toxicity of CPI-203. Consequently, CPI-203 may display several advantages over JQ1. First, CPI-203 exhibited a stronger reactivation activity and an approximately 10-fold lower cytotoxicity than JQ1. The CC<sub>50</sub> values of CPI-203 were higher than 125 μM, which is substantially higher than its active concentration (1 μM). Furthermore, the CC<sub>50</sub> values of CPI-203 toward the two parental cells were higher than those for HIV-1 latent cells, indicating that CPI-203 could kill latently infected HIV-1 cells more specifically than HIV-1-noninfected cells. Our recent research showed that a BET bromodomain inhibitor apabetalone induced the preferential apoptosis of HIV-1 latent cells to promote the death of reactivated reservoir cells. Other studies have also reported that some PKC activators could induce HIV-1 reversal and cell apoptosis in HIV-1 latent cells [40, 41]. In this study, CPI-203 could kill latently infected HIV-1 cells more specifically than HIV-1-noninfected cells, indicating that it is possible to induce cell apoptosis in HIV latent cells and then cause a reduction of the inducible

latent reservoir. Because *in vivo* assays for acute toxicity in mice are time consuming and costly, the possible toxicity of CPI-203 and JQ1 was estimated using TEST. This tool uses different methods to predict toxicity, and the consensus models afford a higher prediction accuracy for the external validation dataset with a higher coverage compared with individual constituent models [42, 43]. The validated consensus LD<sub>50</sub> models developed in this study can be used as reliable computational predictors of *in vivo* acute toxicity. The LD<sub>50</sub> of CPI-203 was 2-fold higher than that of JQ1, indicating that CPI-203 might have minimal cytotoxic effects. Second, according to Lipinski's rule of five, the octanol-water partition coefficient log P value of a promising lead compound should be not greater than 5 [44]. The log P value for CPI-203 was 4.06 and that for JQ1 was 5.85. Third, CPI-203 induced a stronger reactivation in latently infected cell lines than JQ1. Taken together, the results indicate that the absorption of CPI-203 is better than JQ1 and, hence, may have superior clinical value.

The failure of PMA and prostratin in clinical/preclinical trials suggests that the safety of LRA candidates should be evaluated as early as possible [45, 46]. The major problem with PKC agonists is the nonspecific induction of global T cell activation, possibly caused by the systemic release of pro-inflammatory cytokines. Notably, a recent report for a novel LRA showed that a combination of a PKC activator with a BRD4 inhibitor (JQ1) reduced the production of inflammatory cytokines [41]. To evaluate the synergistic effects of CPI-203 and prostratin, we detected whether CPI-203 could reduce the side effects of prostratin by inhibiting the release of inflammatory cytokines. Some researchers have reported that JQ1 impairs mouse macrophage inflammatory responses *in vivo* [36]. Our results showed that CPI-203 inhibited the release of both LPS- and prostratin-stimulated inflammatory cytokines, and the combined treatment of CPI-203 and prostratin could significantly reduce the release prostratin-stimulated inflammatory cytokines *in vitro* or *in vivo*. These results suggest that CPI-203 may be a bifunctional candidate for advancing HIV-1 eradication and benefiting hyperinflammatory conditions during the HIV-induced “cytokine storm”.

Meanwhile, Lucera *et al.* reported that vorinostat, a broad-spectrum HDAC inhibitor, increased the susceptibility of CD4<sup>+</sup> T cells to HIV-1[47]. Our data also showed that the capacity of CPI-203 to reduce the receptor/coreceptor expression on the T cell surface directly impacted the susceptibility of CD4<sup>+</sup> T cells *in vitro* and blocked viral spread to uninfected bystander CD4<sup>+</sup> T cells. As the primary receptor of the HIV-1 envelope glycoprotein 120 (gp120), CD4 is critical for HIV-1 entry into host cells. The fact that the BRD inhibitor downregulates CD4 expression is disconcerting, given the primary role for these cells in human immunity. Recent literature has indicated that blocking the interaction of HIV-1 and its primary receptor CD4 is one strategy for identifying new HIV-1 entry inhibitors or HIV-1 monoclonal antibodies for fighting HIV-1 infection [48]. Our previous studies reported that a series of chemically modified proteins inhibited HIV-1 fusion/entry by targeting both HIV-1 gp120 envelope and CD4 receptor [21, 49]. It is worth noting that ibalizumab, an FDA-approved ART drug for multidrug resistant HIV-1, is a humanized monoclonal antibody that binds to the D2 domain of CD4 with significant anti-HIV-1 activity and minor adverse effects [50]. Ibalizumab cannot directly block the gp120/CD4 interaction, but it induces conformational changes in the CD4-gp120 complex and prevents HIV-1 entry. Another representative compound is cyclotriazadisulfonamide (CADA), a small molecule that can decrease the amount of cell surface and intracellular CD4, thereby resulting in anti-HIV-1 activity [51]. In addition, an HIV-1 latency-reversing agent may be more favorable for avoiding secondary infection by downregulating CD4 expression [29]. Because CD4/CCR5/CXCR4-positive cells play an important role in T cell activation, one of the concerns of the drastic reduction of those positive cells may cause some immunological abnormalities. Therefore, long-term observation of the potential harmful effect of CPI-203 on the mucosal immune system is warranted, and animal studies to evaluate its *in vivo* toxicity will be necessary in the future.

Because of its effective HIV-1 reactivation and low cytotoxicity as well as the beneficial high water solubility of the amino group, CPI-203 promises to be a reasonable choice for accelerating the eradication of the latent HIV-1 reservoir in the

context of cART. Together, these results encouraged us to investigate the mechanism of action of CPI-203 as a potential latency-reversing candidate.

BRD4 was previously identified to be a positive regulatory component of p-TEFb, a kinase composed of the catalytic subunit CDK9 and the regulatory subunit Cyclin T1 [13, 52]. P-TEFb plays a major role in transcriptional elongation by facilitating the continuation of RNA Pol II-mediated transcription after the promoter-proximal pause via the CDK9-mediated phosphorylation of RNA Pol II CTD at Ser2. BRD4 has been verified to compete with HIV-1 Tat for p-TEFb binding at the HIV-1 promoter and inhibit the activation of HIV-1 transcription elongation [23, 53]. CPI-203 is a methyl-triazolo-based BETi with a high affinity for the BRD4 protein, indicating that the CPI-203-mediated transcriptional activation of HIV-1 might be directly attributed to BRD4 dissociating from p-TEFb. In this study, we used the co-IP assay to demonstrate that CPI-203 significantly dissociated the p-TEFb subunits, including CDK9 and Cyclin T1, from BRD4. Furthermore, using ChIP assays, we further found that CPI-203 stimulation promoted CDK9 recruitment directly to the HIV-1 LTR and induced RNAP II CTD phosphorylation and viral transcription. Our results further confirmed that the CPI-203-mediated activation of HIV-1 involved an increase in the phosphorylation of the CDK9 T-loop and the RNA Pol II CTD.

Due to the diversity in establishing and maintaining the latent HIV-1 reservoir, a single LRA might be not be sufficient to affect the multiple signaling regulatory pathways promoting HIV-1 latency [25, 29, 54]. Furthermore, a combination of therapeutics may be beneficial to reduce side effects and delay the generation of drug resistance [16]. Recent studies have shown that a combination of BETis with other types of LRAs, specifically PKC agonists (prostratin, ingenol-B and bryostatin-1), exhibited synergism in the reactivation of latent HIV-1 [55-57]. As expected, our data also showed that a combination of CPI-203 and prostratin or SAHA was substantially more effective at promoting viral expression from latently infected cell models *in vitro* and primary CD4<sup>+</sup> T cells from HIV-1-infected individuals undergoing suppressive cART *ex vivo*. More extensive investigations into the synergistic reactivation of CPI-203 and additional LRA classes and the mechanism underlying

latent HIV-1 expression will be performed in the future.

Generally, an inflammatory response can lead to tissue damage, hemodynamic changes, multiple organ failure and, ultimately, death. Acute or chronically HIV-infected individuals appear to express higher levels of inflammatory cytokines, including IL-6 and TNF- $\alpha$ , in their peripheral blood. Notably, some LARs do not completely reverse/normalize the inflammatory status induced by HIV-1 infection, as a sustained activation of the immune system is observed, which leads to non-HIV-related morbidity. Strikingly, the BETi JQ1 ablates high levels of cytokine production *in vitro* and impairs mouse macrophage inflammatory responses *in vivo* [38]. Therefore, the effect of CPI-203 on inflammation during HIV-1 eradication interventions was evaluated in this study. As previously suggested, prostratin induces a “cytokine storm”, the severe, systemic production of inflammatory cytokines dominated by macrophages in response to endotoxemic shock [45, 58]. Our results showed that CPI-203 significantly inhibited the release of both LPS- and prostratin-stimulated inflammatory cytokines *in vitro* and *in vivo*, suggesting that it may be a new bifunctional candidate for improving HIV-1 eradication and benefiting hyperinflammatory conditions during HIV-induced “cytokine storms”. Collectively, our results demonstrate that CPI-203 is a promising, safe LRA candidate for the design of targeted strategies to “shock and kill” HIV-1 and, thus, represents a potential functional cure. CPI-203 plays an important role in inducing RNA Pol II CTD phosphorylation via the p-TEFb pathway to regulate HIV-1 LTR gene expression and has good potency for use in combination with anti-HIV drugs to permanently cure HIV-1 infection.

### **Conflicts of interest**

None of the authors have any conflicts of interest to declare.

### **Acknowledgements**

We thank Dr. Shibo Jiang and Dr. Lu Lu of Fudan University, China, for providing the latently infected cell lines. This study was supported by the Natural Science

Foundation of China (81673481 to L.L. and 81773787 to S.L.) and the Guangzhou Baiyun District Science and Technology Program Project (2016-KJ-002 to L.L.).

ACCEPTED MANUSCRIPT



## References

- [1] R.T. Davey, Jr., N. Bhat, C. Yoder, T.W. Chun, J.A. Metcalf, R. Dewar, et al., HIV-1 and T cell dynamics after interruption of highly active antiretroviral therapy (HAART) in patients with a history of sustained viral suppression, *Proceedings of the National Academy of Sciences of the United States of America*, 96 (1999) 15109-15114.
- [2] B.M. Peterlin, D. Trono, Hide, shield and strike back: how HIV-infected cells avoid immune eradication, *Nature reviews. Immunology*, 3 (2003) 97-107.
- [3] N.M. Archin, D.M. Margolis, Emerging strategies to deplete the HIV reservoir, *Current opinion in infectious diseases*, 27 (2014) 29-35.
- [4] A.J. Kandathil, S. Sugawara, A. Balagopal, Erratum to: Are T cells the only HIV-1 reservoir?, *Retrovirology*, 14 (2017) 11.
- [5] S.G. Deeks, S.R. Lewin, A.L. Ross, J. Ananworanich, M. Benkirane, P. Cannon, et al., International AIDS Society global scientific strategy: towards an HIV cure 2016, *Nature medicine*, 22 (2016) 839-850.
- [6] M.C. Pitman, J.S.Y. Lau, J.H. McMahon, S.R. Lewin, Barriers and strategies to achieve a cure for HIV, *The lancet. HIV*, 5 (2018) e317-e328.
- [7] S. Sengupta, R.F. Siliciano, Targeting the Latent Reservoir for HIV-1, *Immunity*, 48 (2018) 872-895.
- [8] T.A. Rasmussen, M. Tolstrup, A. Winckelmann, L. Ostergaard, O.S. Sogaard, Eliminating the latent HIV reservoir by reactivation strategies: advancing to clinical trials, *Human vaccines & immunotherapeutics*, 9 (2013) 790-799.
- [9] H.T. Shang, J.W. Ding, S.Y. Yu, T. Wu, Q.L. Zhang, F.J. Liang, Progress and challenges in the use of latent HIV-1 reactivating agents, *Acta pharmacologica Sinica*, 36 (2015) 908-916.
- [10] C. Banerjee, N. Archin, D. Michaels, A.C. Belkina, G.V. Denis, J. Bradner, et al., BET bromodomain inhibition as a novel strategy for reactivation of HIV-1, *Journal of leukocyte biology*, 92 (2012) 1147-1154.
- [11] K. Bartholomeeusen, Y. Xiang, K. Fujinaga, B.M. Peterlin, Bromodomain and extra-terminal (BET) bromodomain inhibition activate transcription via transient release of positive transcription elongation factor b (P-TEFb) from 7SK small nuclear ribonucleoprotein, *The Journal of biological chemistry*, 287 (2012) 36609-36616.
- [12] P. Filippakopoulos, J. Qi, S. Picaud, Y. Shen, W.B. Smith, O. Fedorov, et al., Selective inhibition of BET bromodomains, *Nature*, 468 (2010) 1067-1073.
- [13] M.K. Jang, K. Mochizuki, M. Zhou, H.S. Jeong, J.N. Brady, K. Ozato, The bromodomain protein

Brd4 is a positive regulatory component of P-TEFb and stimulates RNA polymerase II-dependent transcription, *Molecular cell*, 19 (2005) 523-534.

[14] D. Boehm, V. Calvanese, R.D. Dar, S. Xing, S. Schroeder, L. Martins, et al., BET bromodomain-targeting compounds reactivate HIV from latency via a Tat-independent mechanism, *Cell cycle (Georgetown, Tex.)*, 12 (2013) 452-462.

[15] R.J. Conrad, P. Fozouni, S. Thomas, H. Sy, Q. Zhang, M.M. Zhou, et al., The Short Isoform of BRD4 Promotes HIV-1 Latency by Engaging Repressive SWI/SNF Chromatin-Remodeling Complexes, *Molecular cell*, 67 (2017) 1001-1012.e1006.

[16] P. Lu, X. Qu, Y. Shen, Z. Jiang, P. Wang, H. Zeng, et al., The BET inhibitor OTX015 reactivates latent HIV-1 through P-TEFb, *Scientific reports*, 6 (2016) 24100.

[17] Z. Li, J. Guo, Y. Wu, Q. Zhou, The BET bromodomain inhibitor JQ1 activates HIV latency through antagonizing Brd4 inhibition of Tat-transactivation, *Nucleic acids research*, 41 (2013) 277-287.

[18] T. Diaz, V. Rodriguez, E. Lozano, M.P. Mena, M. Calderon, L. Rosinol, et al., The BET bromodomain inhibitor CPI203 improves lenalidomide and dexamethasone activity in in vitro and in vivo models of multiple myeloma by blockade of Ikaros and MYC signaling, *Haematologica*, 102 (2017) 1776-1784.

[19] M.B. Siegel, S.Q. Liu, M.A. Davare, S.E. Spurgeon, M.M. Loriaux, B.J. Druker, et al., Small molecule inhibitor screen identifies synergistic activity of the bromodomain inhibitor CPI203 and bortezomib in drug resistant myeloma, *Oncotarget*, 6 (2015) 18921-18932.

[20] A. Moros, V. Rodriguez, I. Saborit-Villarroya, A. Montraveta, P. Balsas, P. Sandy, et al., Synergistic antitumor activity of lenalidomide with the BET bromodomain inhibitor CPI203 in bortezomib-resistant mantle cell lymphoma, *Leukemia*, 28 (2014) 2049-2059.

[21] L. Li, P. Qiao, J. Yang, L. Lu, S. Tan, H. Lu, et al., Maleic anhydride-modified chicken ovalbumin as an effective and inexpensive anti-HIV microbicide candidate for prevention of HIV sexual transmission, *Retrovirology*, 7 (2010) 37.

[22] J. Chen, R. Ren, F. Yu, C. Wang, X. Zhang, W. Li, et al., A Degraded Fragment of HIV-1 Gp120 in Rat Hepatocytes Forms Fibrils and Enhances HIV-1 Infection, *Biophysical journal*, 113 (2017) 1425-1439.

[23] X.X. Zhang, J. Lin, T.Z. Liang, H. Duan, X.H. Tan, B.M. Xi, et al., The BET bromodomain inhibitor apabetalone induces apoptosis of latent HIV-1 reservoir cells following viral reactivation, *Acta pharmacologica Sinica*, 40 (2019) 98-110.

[24] X. Zeng, X. Pan, X. Xu, J. Lin, F. Que, Y. Tian, Resveratrol Reactivates Latent HIV through Increasing Histone Acetylation and Activating Heat Shock Factor 1, 65 (2017) 4384-4394.

[25] G.M. Laird, C.K. Bullen, D.I. Rosenbloom, A.R. Martin, A.L. Hill, C.M. Durand, et al., Ex vivo analysis identifies effective HIV-1 latency-reversing drug combinations, *The Journal of clinical*

investigation, 125 (2015) 1901-1912.

[26] A. Jordan, D. Bisgrove, E. Verdin, HIV reproducibly establishes a latent infection after acute infection of T cells in vitro, *The EMBO journal*, 22 (2003) 1868-1877.

[27] K.A. Clouse, D. Powell, I. Washington, G. Poli, K. Strebel, W. Farrar, et al., Monokine regulation of human immunodeficiency virus-1 expression in a chronically infected human T cell clone, *Journal of immunology* (Baltimore, Md. : 1950), 142 (1989) 431-438.

[28] S. Emiliani, W. Fischle, M. Ott, C. Van Lint, C.A. Amella, E. Verdin, Mutations in the tat gene are responsible for human immunodeficiency virus type 1 postintegration latency in the U1 cell line, *Journal of virology*, 72 (1998) 1666-1670.

[29] G. Jiang, E.A. Mendes, P. Kaiser, D.P. Wong, Y. Tang, I. Cai, et al., Synergistic Reactivation of Latent HIV Expression by Ingenol-3-Angelate, PEP005, Targeted NF- $\kappa$ B Signaling in Combination with JQ1 Induced p-TEFb Activation, *PLoS pathogens*, 11 (2015) e1005066.

[30] G. Jiang, S. Dandekar, Targeting NF-kappaB signaling with protein kinase C agonists as an emerging strategy for combating HIV latency, *AIDS research and human retroviruses*, 31 (2015) 4-12.

[31] H.C. Yang, S. Xing, L. Shan, K. O'Connell, J. Dinoso, A. Shen, et al., Small-molecule screening using a human primary cell model of HIV latency identifies compounds that reverse latency without cellular activation, *The Journal of clinical investigation*, 119 (2009) 3473-3486.

[32] K. Benamar, M. Yondorf, E.B. Geller, T.K. Eisenstein, M.W. Adler, Physiological evidence for interaction between the HIV-1 co-receptor CXCR4 and the cannabinoid system in the brain, *British journal of pharmacology*, 157 (2009) 1225-1231.

[33] R. Chen, Z. Yang, Q. Zhou, Phosphorylated positive transcription elongation factor b (P-TEFb) is tagged for inhibition through association with 7SK snRNA, *The Journal of biological chemistry*, 279 (2004) 4153-4160.

[34] N. He, N.S. Jahchan, E. Hong, Q. Li, M.A. Bayfield, R.J. Maraia, et al., A La-related protein modulates 7SK snRNP integrity to suppress P-TEFb-dependent transcriptional elongation and tumorigenesis, *Molecular cell*, 29 (2008) 588-599.

[35] F. Itzen, A.K. Greifenberg, C.A. Bosken, M. Geyer, Brd4 activates P-TEFb for RNA polymerase II CTD phosphorylation, *Nucleic acids research*, 42 (2014) 7577-7590.

[36] M.M. Freeman, M.S. Seaman, S. Rits-Volloch, X. Hong, C.Y. Kao, D.D. Ho, et al., Crystal structure of HIV-1 primary receptor CD4 in complex with a potent antiviral antibody, *Structure* (London, England : 1993), 18 (2010) 1632-1641.

[37] S. Meng, L. Zhang, Y. Tang, Q. Tu, L. Zheng, L. Yu, et al., BET Inhibitor JQ1 Blocks Inflammation and Bone Destruction, *Journal of dental research*, 93 (2014) 657-662.

[38] M. Huang, S. Zeng, Y. Zou, M. Shi, Q. Qiu, Y. Xiao, et al., The suppression of bromodomain and

extra-terminal domain inhibits vascular inflammation by blocking NF-kappaB and MAPK activation, *British journal of pharmacology*, 174 (2017) 101-115.

[39] K.M. Barton, B.D. Burch, N. Soriano-Sarabia, D.M. Margolis, Prospects for treatment of latent HIV, *Clinical pharmacology and therapeutics*, 93 (2013) 46-56.

[40] S.I. Hattori, K. Matsuda, K. Tsuchiya, H. Gatanaga, S. Oka, K. Yoshimura, et al., Combination of a Latency-Reversing Agent With a Smac Mimetic Minimizes Secondary HIV-1 Infection in vitro, *Frontiers in microbiology*, 9 (2018) 2022.

[41] K. Matsuda, T. Kobayakawa, K. Tsuchiya, S.I. Hattori, W. Nomura, H. Gatanaga, et al., Benzolactam-related compounds promote apoptosis of HIV-infected human cells via protein kinase C-induced HIV latency reversal, *The Journal of biological chemistry*, 294 (2019) 116-129.

[42] H. Zhu, T.M. Martin, L. Ye, A. Sedykh, D.M. Young, A. Tropsha, Quantitative structure-activity relationship modeling of rat acute toxicity by oral exposure, *Chemical research in toxicology*, 22 (2009) 1913-1921.

[43] A. Cassano, A. Manganaro, T. Martin, D. Young, N. Piclin, M. Pintore, et al., CAESAR models for developmental toxicity, *Chemistry Central journal*, 4 Suppl 1 (2010) S4.

[44] C.A. Lipinski, Lead- and drug-like compounds: the rule-of-five revolution, *Drug discovery today. Technologies*, 1 (2004) 337-341.

[45] C. Dental, A. Proust, HIV-1 Latency-Reversing Agents Prostratin and Bryostatin-1 Induce Blood-Brain Barrier Disruption/Inflammation and Modulate Leukocyte Adhesion/Transmigration, 198 (2017) 1229-1241.

[46] A. Biancotto, J.C. Grivel, F. Gondois-Rey, L. Bettendroffer, R. Vigne, S. Brown, et al., Dual role of prostratin in inhibition of infection and reactivation of human immunodeficiency virus from latency in primary blood lymphocytes and lymphoid tissue, *Journal of virology*, 78 (2004) 10507-10515.

[47] M.B. Lucera, C.A. Tilton, H. Mao, C. Dobrowolski, C.O. Tabler, A.A. Haqqani, et al., The histone deacetylase inhibitor vorinostat (SAHA) increases the susceptibility of uninfected CD4+ T cells to HIV by increasing the kinetics and efficiency of postentry viral events, *Journal of virology*, 88 (2014) 10803-10812.

[48] C. Zhang, H. Zhang, L.S. Huang, S. Zhu, Y. Xu, X.Q. Zhang, et al., Virtual Screening, Biological Evaluation, and 3D-QSAR Studies of New HIV-1 Entry Inhibitors That Function via the CD4 Primary Receptor, *Molecules (Basel, Switzerland)*, 23 (2018) doi: 10.3390/molecules23113036.

[49] X. Zhang, J. Chen, F. Yu, C. Wang, R. Ren, Q. Wang, et al., 3-Hydroxyphthalic Anhydride-Modified Rabbit Anti-PAP IgG as a Potential Bifunctional HIV-1 Entry Inhibitor, *Frontiers in microbiology*, 9 (2018) 1330.

[50] S.A. Iacob, D.G. Iacob, Ibalizumab Targeting CD4 Receptors, An Emerging Molecule in HIV Therapy, *Frontiers in microbiology*, 8 (2017) 2323.

- [51] K. Vermeire, K. Princen, S. Hatse, E. De Clercq, K. Dey, T.W. Bell, et al., CADA, a novel CD4-targeted HIV inhibitor, is synergistic with various anti-HIV drugs in vitro, *AIDS (London, England)*, 18 (2004) 2115-2125.
- [52] Z. Yang, J.H. Yik, R. Chen, N. He, M.K. Jang, K. Ozato, et al., Recruitment of P-TEFb for stimulation of transcriptional elongation by the bromodomain protein Brd4, *Molecular cell*, 19 (2005) 535-545.
- [53] L.S. Weinberger, J.C. Burnett, J.E. Toettcher, A.P. Arkin, D.V. Schaffer, Stochastic gene expression in a lentiviral positive-feedback loop: HIV-1 Tat fluctuations drive phenotypic diversity, *Cell*, 122 (2005) 169-182.
- [54] R. Olesen, S. Vigano, T.A. Rasmussen, O.S. Sogaard, Z. Ouyang, M. Buzon, et al., Innate Immune Activity Correlates with CD4 T Cell-Associated HIV-1 DNA Decline during Latency-Reversing Treatment with Panobinostat, *Journal of virology*, 89 (2015) 10176-10189.
- [55] S.A. Williams, L.F. Chen, H. Kwon, D. Fenard, D. Bisgrove, E. Verdin, et al., Prostratin antagonizes HIV latency by activating NF-kappaB, *The Journal of biological chemistry*, 279 (2004) 42008-42017.
- [56] G. Jiang, E.A. Mendes, P. Kaiser, S. Sankaran-Walters, Y. Tang, M.G. Weber, et al., Reactivation of HIV latency by a newly modified Ingenol derivative via protein kinase Cdelta-NF-kappaB signaling, *AIDS (London, England)*, 28 (2014) 1555-1566.
- [57] C. Dental, A. Proust, M. Ouellet, C. Barat, M.J. Tremblay, HIV-1 Latency-Reversing Agents Prostratin and Bryostatins Induce Blood-Brain Barrier Disruption/Inflammation and Modulate Leukocyte Adhesion/Transmigration, *Journal of immunology (Baltimore, Md. : 1950)*, 198 (2017) 1229-1241.
- [58] S. Ahir, J. Mania-Pramanik, V. Chavan, S. Kerkar, P. Samant-Mavani, R. Nanavati, et al., Genetic variation in the promoter region of pro-inflammatory cytokine TNF-alpha in perinatal HIV transmission from Mumbai, India, *Cytokine*, 72 (2015) 25-30.

## Figure legends

**Fig. 1. CPI-203 induces HIV-1 expression in latently infected cell lines in a dose- and time-dependent manner.** J-Lat A2 (A) and J-Lat 10.6 (C) cells were treated with CPI-203 at the indicated concentrations for 48 h. The percentage of GFP-positive cells within the entire population was measured by flow cytometry. The magnitude of reactivation induced by 10 ng/ml of PMA was defined as 100% reactivation, and the data are representative fold reactivation over PMA. J-Lat A2 (B) and J-Lat 10.6 (D) cells were treated with 1  $\mu$ M CPI-203 for the indicated time period. The percentage of GFP-positive cells within the entire population was measured by flow cytometry. ACH2 cells were treated with CPI-203 at the indicated concentrations (E) or for the indicated amounts of time (F). The p24 antigen was detected by ELISA. The data are representative of three independent experiments (mean  $\pm$  SD). One-way ANOVA followed by Dunnett's multiple comparison post hoc test was used to statistically analyze the differences between the CPI-203 and solvent mock groups (\* $p$  < 0.05, \*\* $p$  < 0.01).

**Fig. 2. CPI-203 activates HIV-1 transcription *ex vivo* and HIV-1 transcriptional gene expression *in vitro*.** (A) Resting CD4<sup>+</sup> T cells were isolated from HIV-1-infected patients undergoing suppressive cART and treated with CPI-203 (1  $\mu$ M), JQ1 (2  $\mu$ M), SAHA (1  $\mu$ M) and prostratin (1  $\mu$ M) for 48 h. (B) ACH2 cells were treated with CPI-203 at the indicated concentrations for 48 h. Total mRNA was extracted, HIV-1 RNA levels were quantified by RT-qPCR, and fold increases were determined relative to those in the solvent control group. The data are a combination of three independent experiments (mean  $\pm$  SD,  $p$  values were obtained by one-way ANOVA, \* $p$  < 0.05, \*\* $p$  < 0.01).

**Fig. 3. CPI-203 does not induce global activation or pro-inflammatory cytokine release and downregulates the cell surface expression of HIV-1 receptor/coreceptors.** PBMCs were isolated from healthy HIV-negative donors and treated with prostratin (1  $\mu$ M) and CPI-203 (1  $\mu$ M) for 24 (A) or 72 h (B). The expression profiles of the cell activation markers CD69, CD38, CD25 and HLA-DR

were detected by flow cytometry. **(C)** The effects of CPI-203 on the expression of pro-inflammatory cytokines, including IL-2, IL-6, TNF- $\alpha$  and IFN- $\gamma$ , in PBMCs were analyzed by ELISA. One-way ANOVA followed by Dunnett's multiple comparison post hoc test was used to statistically analyze the differences between the CPI-203 and mock groups ( $*p < 0.05$ ,  $**p < 0.01$ ). The effects of CPI-203 (1  $\mu$ M) on the expression profiles of CD4, CXCR4 **(D)** and CCR5 **(E)** were determined by flow cytometry.

**Fig. 4. CPI-203 promotes HIV-1 transcription via p-TEFb.**

ACH2 cells were treated with CPI-203 at the indicated concentrations for 48 h **(A)** or for different amounts of time at 1  $\mu$ M **(B)**. The expression levels of CDK9, p-CDK9, Cyclin T1, RNA Pol II CTD, CTD-Ser2p and p24 were analyzed by WB. The expression level of  $\beta$ -actin was used as a loading control, and the expression of p24 indicated the reactivation of HIV-1. The quantifications of CDK9, CDK9 phosphorylation on Thr186, CTD-Ser2p and p24 in **A** and **B** were performed in **(C)** and **(D)**. Data represent the mean  $\pm$  SD of three independent experiments.  $*p < 0.05$ ,  $**p < 0.01$  vs Mock treatment.

**Fig. 5. CPI-203 dissociates the p-TEFb complex from BRD4 and increases p-TEFb recruitment to the HIV-1 LTR.**

**(A)** ACH2 cells were stimulated with CPI-203 (1  $\mu$ M) or JQ1 (1  $\mu$ M) for 48 h. Recruitment of the p-TEFb complex by BRD4 was detected by co-IP. **(B)** ACH2 cells were mock-treated or stimulated with CPI-203 (1  $\mu$ M) or JQ1 (1  $\mu$ M) for 48 h. ChIP assays were performed using antibodies against BRD4, CDK9, Pol II CTD-Ser2P or normal rabbit IgG. PCR primers specific for the LTR promoter were used to amplify the DNA isolated from the immunoprecipitated chromatin as described in the Methods section. Each ChIP experiment was repeated three times to confirm the reproducibility of the results. Real-time quantitation of the fold change relative to the mock is shown.  $*p < 0.05$ ,  $**p < 0.01$ .

**Fig. 6. Synergetic reactivation of latent HIV-1 production by CPI-203 combined with other LRAs.**

J-Lat A2 **(A)** and ACH2 **(B)** cells were treated with PMA (10 ng/ml), CPI-203 (0.1  $\mu$ M), prostratin (0.5  $\mu$ M), SAHA (0.5  $\mu$ M) or their combinations

for 48 h. The percentage of GFP-positive cells or the p24 antigen was measured by flow cytometry or ELISA. Data represent the mean  $\pm$  SD of three independent experiments.  $*p < 0.05$ ,  $**p < 0.01$  compared with mock treatment. CPI-203 synergizes with other LRAs to significantly increase GFP-positive cells or the HIV-1 p24 antigen in J-Lat A2 (C) or ACH2 (D) cell lines. The Bliss independence model was used to calculate the synergy of LRA combinations.  $\Delta f_{axy} = 0$  indicates additive effect. Synergy is defined as  $\Delta f_{axy} > 0$  while  $\Delta f_{axy} < 0$  indicates antagonism. Statistical significance was calculated using paired *t* test comparing the experimentally observed and predicated fractional effect. (E) Resting CD4<sup>+</sup> T cells were isolated from HIV-1-infected patients undergoing suppressive cART and treated with CPI-203 (0.1  $\mu$ M), prostratin (0.5  $\mu$ M), SAHA (0.5  $\mu$ M) or their combinations for 48 h. Total mRNA levels were quantified using RT-qPCR, and fold increases were determined relative to those in the LRA control ( $*p < 0.05$ ,  $**p < 0.01$ ).

**Fig. 7. CPI-203 decreases the release of inflammatory cytokines *in vitro*.** The prostratin- (A, C) or LPS-induced (B, D) production of IL-1 $\beta$ , IL-6, TNF- $\alpha$  and MCP-1 in THP-1 cells was detected by RT-qPCR (A, B) or ELISA (C, D). The data are presented as the mean  $\pm$  SD. One-way ANOVA followed by Dunnett's multiple comparison *post hoc* test was used to statistically analyze differences between the prostratin- or LPS-treated group and their combinations with CPI-203 ( $**p < 0.01$ ).

**Fig. 8. CPI-203 reduces the secretion of inflammatory cytokines and ameliorates lung damage.** (A) The secretion of plasma inflammatory cytokines was detected by ELISA. The data are presented as the mean  $\pm$  SD. One-way ANOVA followed by Dunnett's multiple comparison *post hoc* test was used to statistically analyze differences between the control and LPS groups ( $**p < 0.01$ ) and between the LPS and LPS + CPI-203 groups ( $^{##}p < 0.01$ ). (B) H&E-staining and immunohistochemical analysis of lung tissue sections from the indicated group ( $\times 200$ ). N = 5 mice per group.



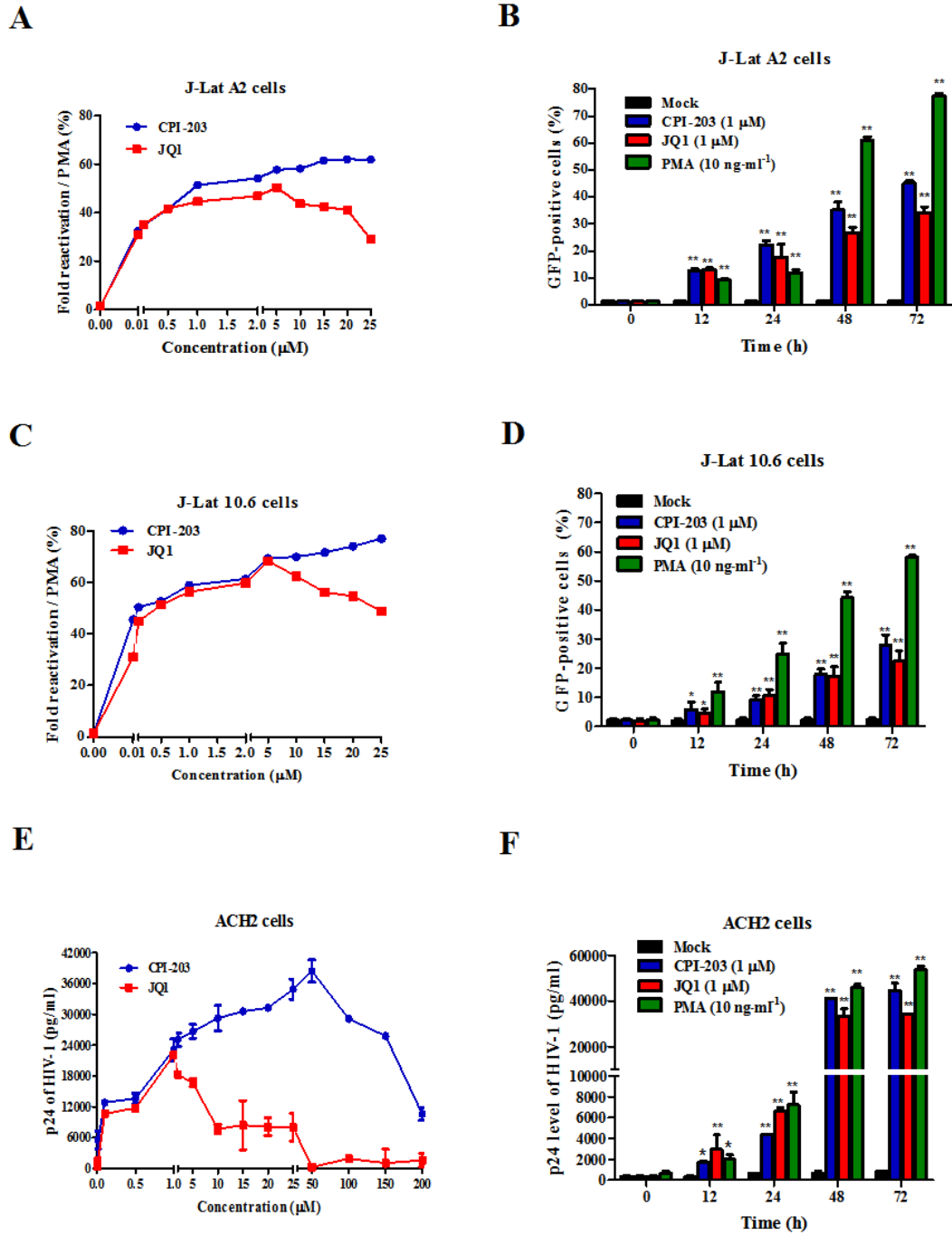


Fig. 1

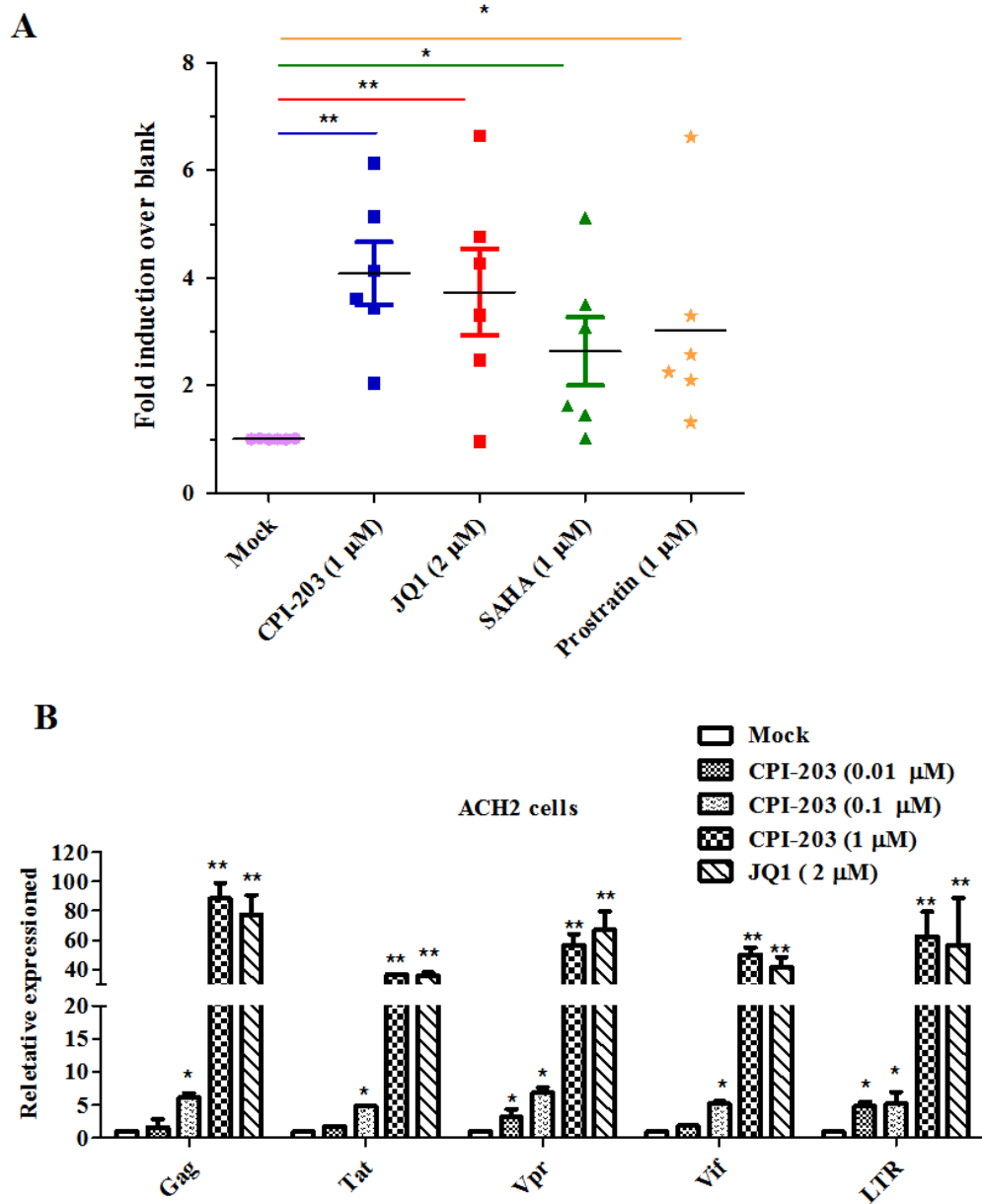


Fig. 2

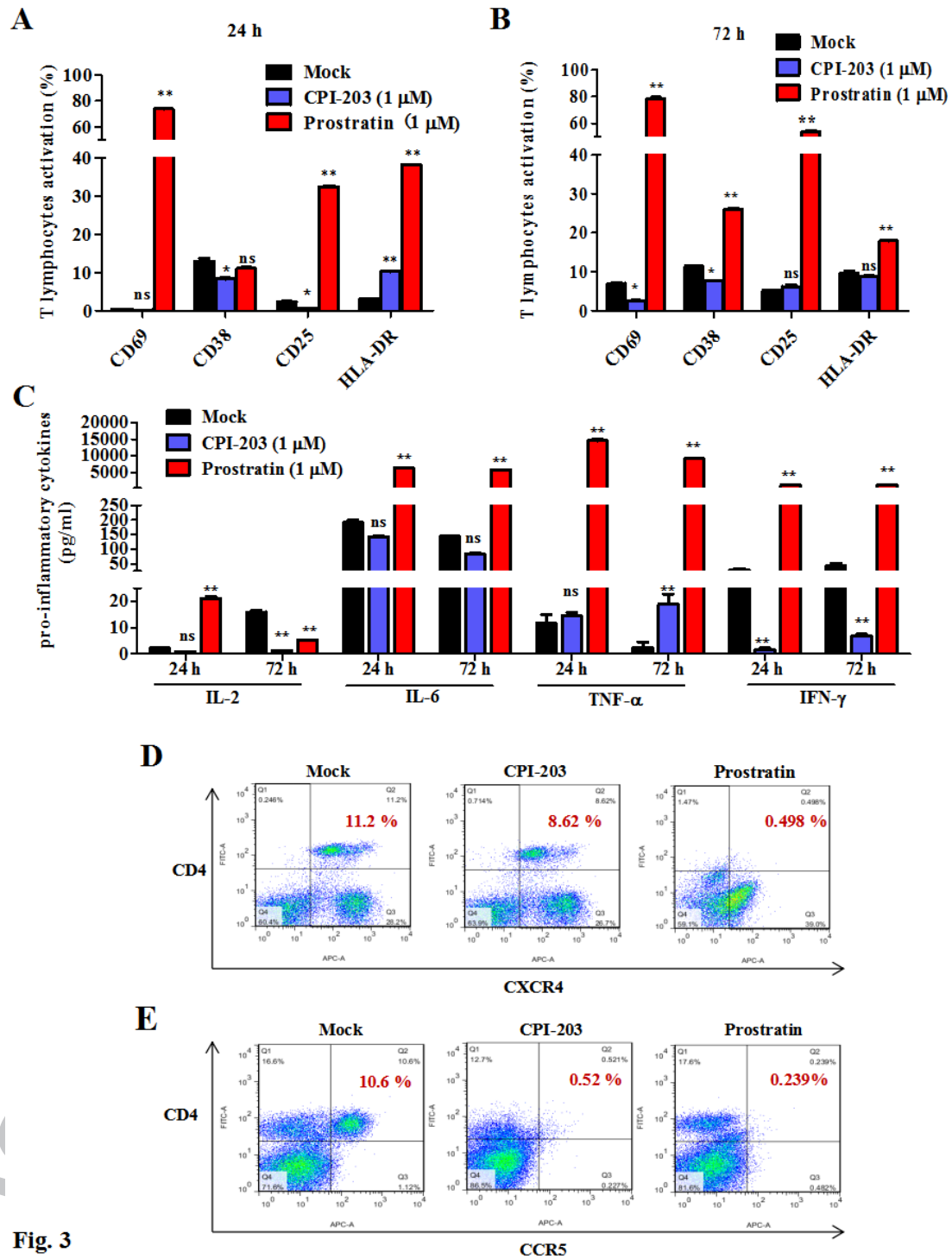


Fig. 3

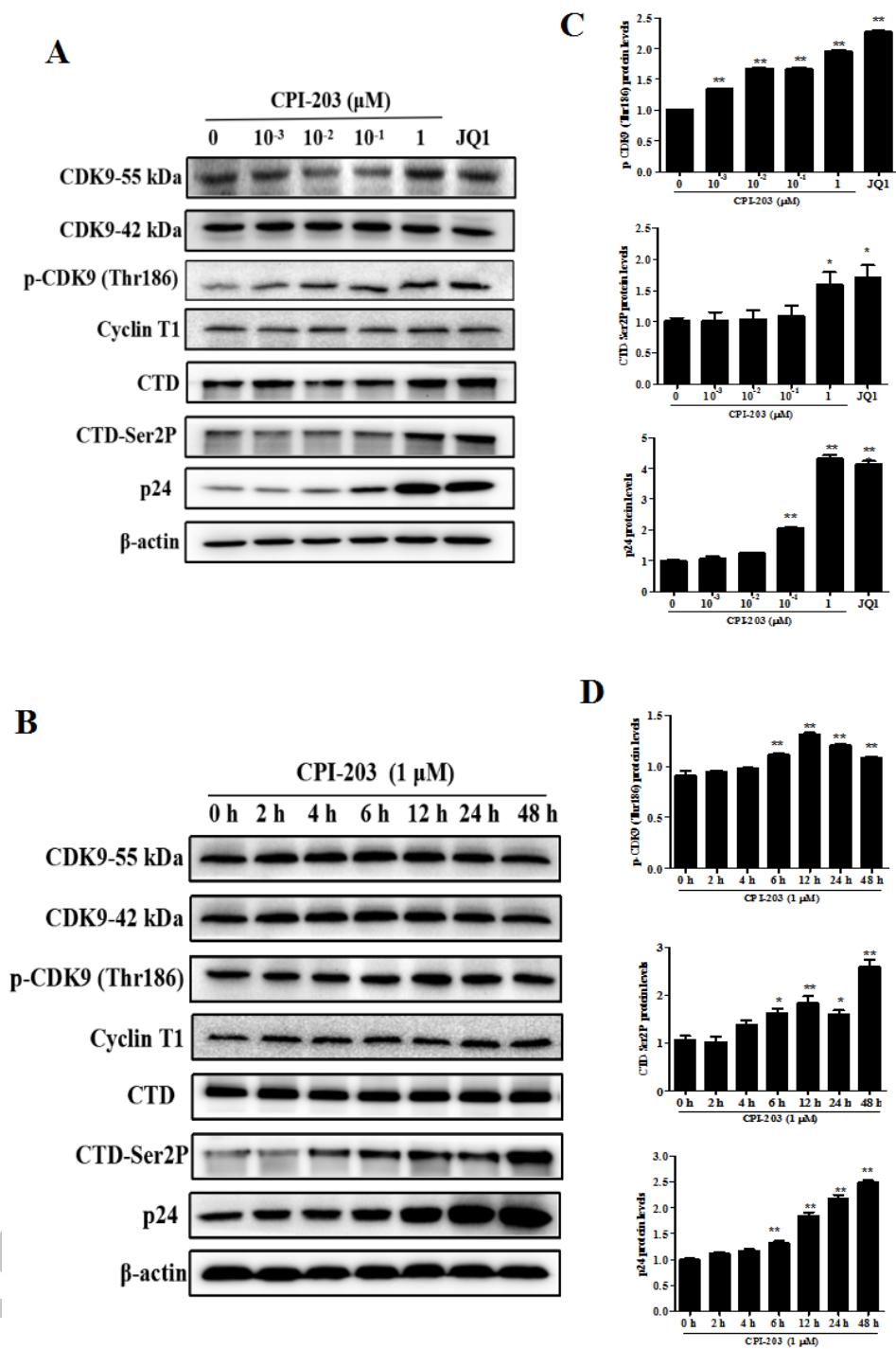


Fig. 4

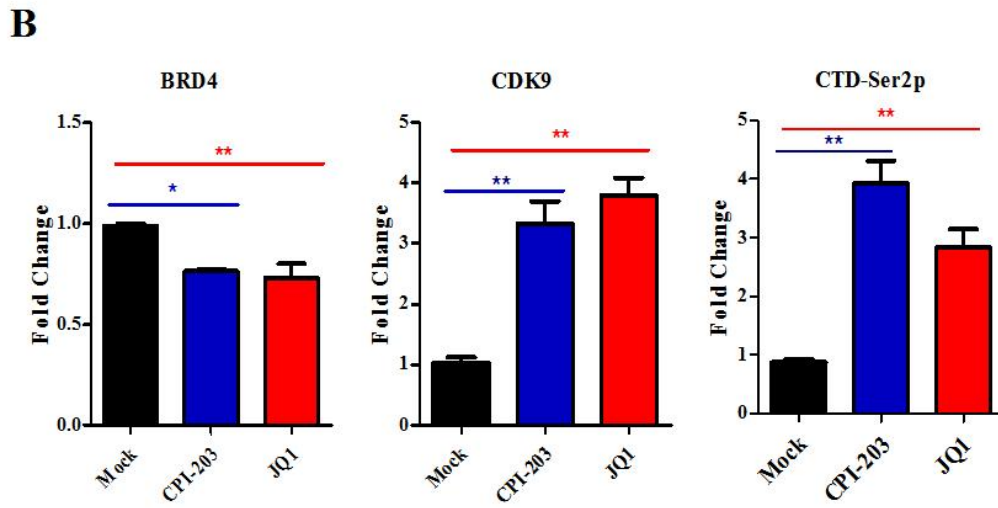
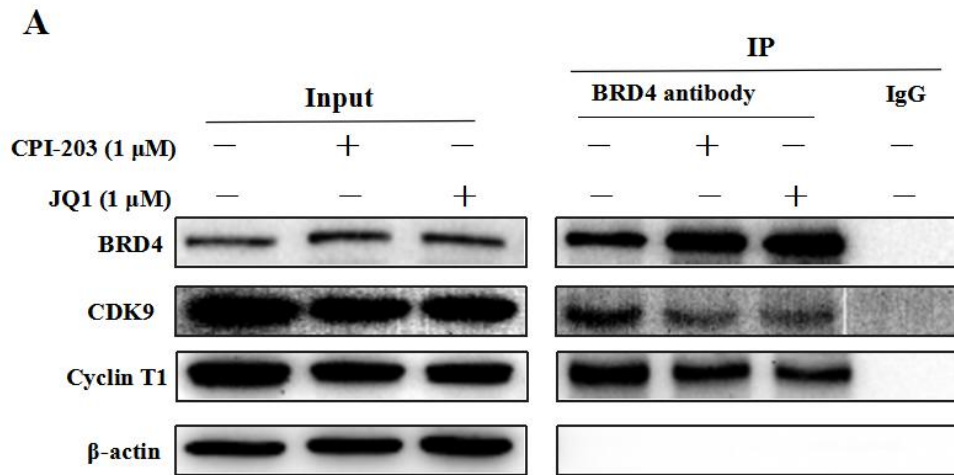


Fig. 5

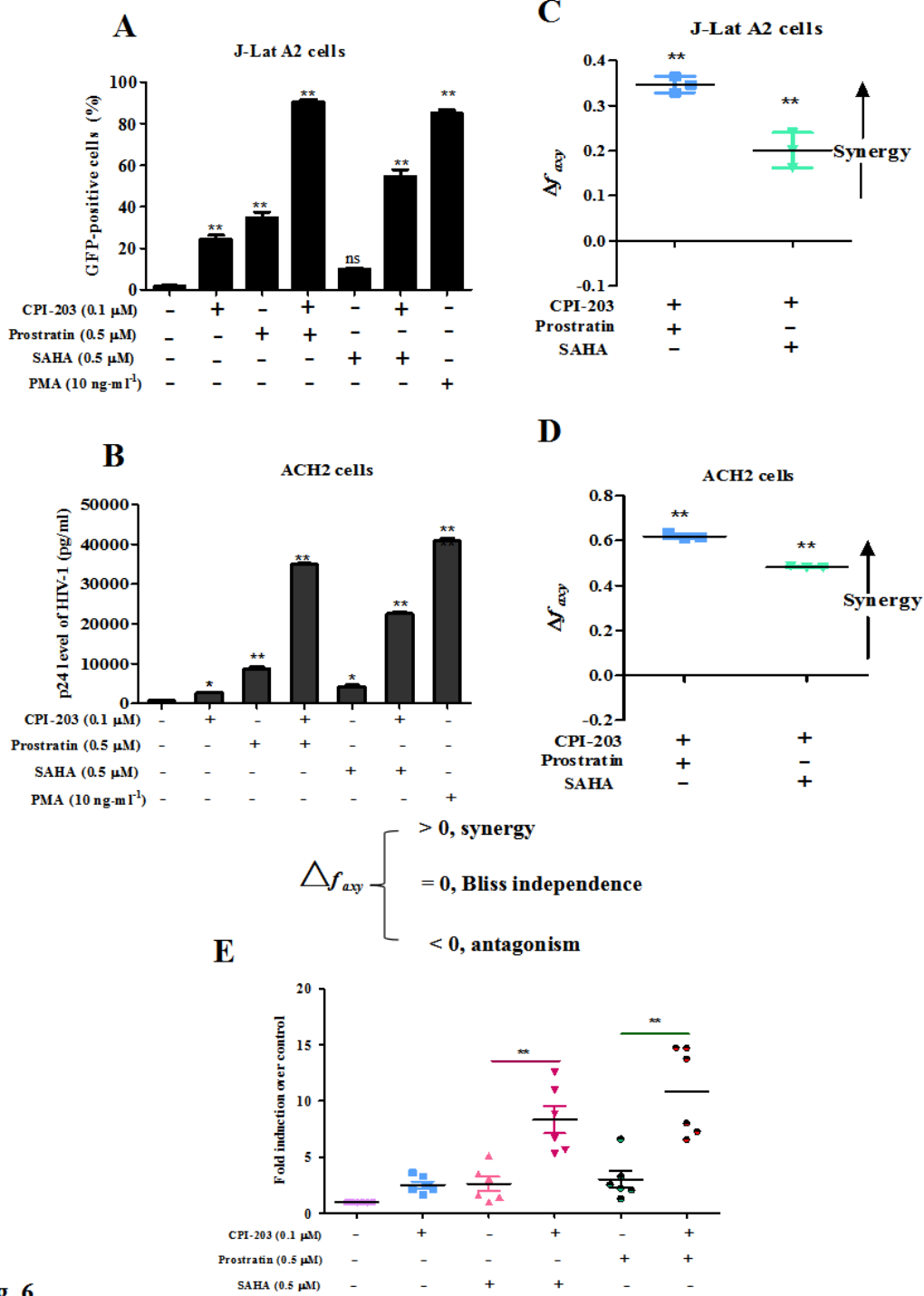


Fig. 6

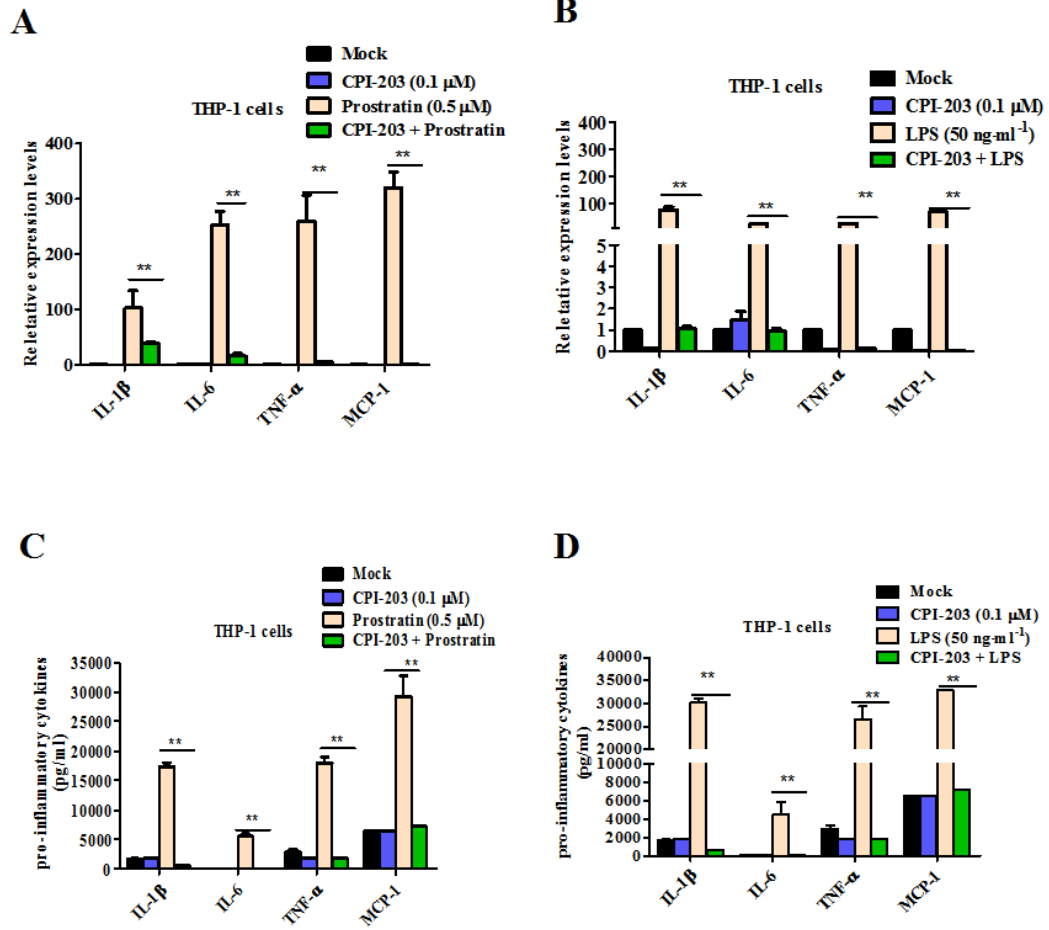


Fig. 7

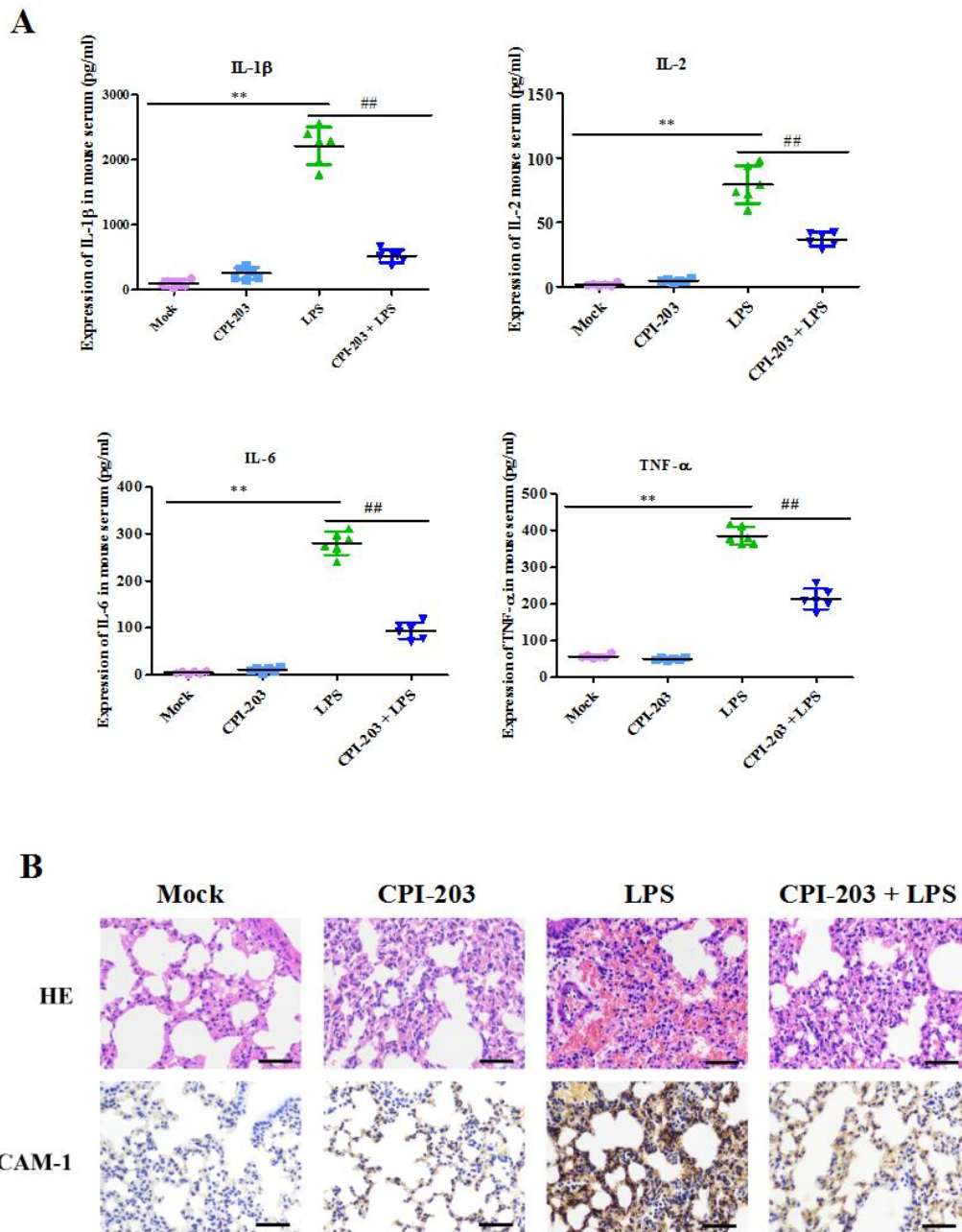


Fig. 8



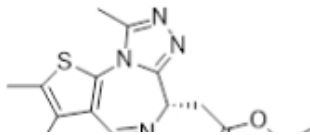
**Table 1. Clinical characteristics of HIV-positive individuals employed in this study**

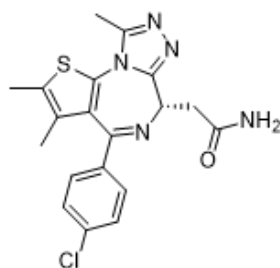
<b>Number</b>	<b>Sex</b>	<b>Age</b>	<b>CD4 count</b>	<b>Time under ART (years)</b>	<b>Viral load (copies/ml)</b>
<b>1</b>	<b>F</b>	<b>39</b>	<b>357</b>	<b>4</b>	<b>&lt; 20</b>
<b>2</b>	<b>M</b>	<b>45</b>	<b>420</b>	<b>2</b>	<b>&lt; 20</b>
<b>3</b>	<b>M</b>	<b>45</b>	<b>708</b>	<b>2.5</b>	<b>&lt; 20</b>
<b>4</b>	<b>M</b>	<b>48</b>	<b>355</b>	<b>6</b>	<b>&lt; 20</b>
<b>5</b>	<b>F</b>	<b>40</b>	<b>588</b>	<b>5</b>	<b>&lt; 20</b>
<b>6</b>	<b>M</b>	<b>52</b>	<b>360</b>	<b>2</b>	<b>&lt; 20</b>

**Table 2. RT-PCR primer sequences**

Sequences		
GAPDH	Forward	CTCTGCTCCTCCTGTTTCGAC
	Reverse	AGTTAAAAGCAGCCCTGGTGA
Gag	Forward	GTCCAGAATGCGAACCCAGA
	Reverse	GTTACGTGCTGGCTCATTGC
Tat	Forward	ATGGAGCCAGTAGATCCTAGACT
	Reverse	CGCTTCTTCCTGCCATAGGA
Vpr	Forward	CCACAAAGGGAGCCATAACAATG
	Reverse	TTATGGCTTCCACTCCTGCC
Vif	Forward	CACACAAGTAGACCCTGACCT
	Reverse	CCCTACCTTGTTATGTCCTGCT
LTR	Forward	GCCTCCTAGCATTTCGTCACAT
	Reverse	GCTGCTTATATGTAGCATCTGAGG
MCP-1	Forward	CAGCCAGATGCAATCAATGCC
	Reverse	TGGAATCCTGAACCCACTTCT
TNF- $\alpha$	Forward	GCCCATGTTGTAGCAAACCC
	Reverse	GGACCTGGGAGTAGATGAGGT
IL-1 $\beta$	Forward	CAACAGGCTGCTCTGGGATT
	Reverse	GGGCCATCAGCTTCAAAGAAC
IL-10	Forward	TGCCAAGCCTTGTCTGAGAT
	Reverse	GAAGAAATCGATGACAGCGCC
IL-6	Forward	AATAACCACCCCTGACCCAAC
	Reverse	TGCTACATTTGCCGAAGAGC
CD4	Forward	AATGAACCGGGGAGTCCCTT
	Reverse	GCTCTTCTTCTGGGAAGCTGT
CXCR4	Forward	GCAGCAGGTAGCAAAGTGAC
	Reverse	CCTTCATGGAGTCATAGTCCCC
CCR5	Forward	TTCTGGGCTCCCTACAACATT
	Reverse	TTGGTCCAACCTGTTAGAGCTA

**Table 3. CPI-203 displays minimal toxicity and good lipophilicity**

CPI-203	JQ1
	



Cells	CC <sub>50</sub> (μM, mean ± SD) <sup>a</sup>	
PBMCs	301.70 ± 61.23	31.27 ± 2.74
J-Lat A2	197.10 ± 3.89	22.79 ± 0.63
J-Lat 10.6	124.94 ± 15.62	23.73 ± 2.30
ACH2	209.67 ± 5.12	25.41 ± 0.72
Jurkat	291.77 ± 7.95	31.41 ± 1.10
A3.01	358.17 ± 10.08	43.42 ± 0.60

Lipophilicity		
Log P <sub>o/w</sub>	4.06	5.85

Methods	Oral rat LD <sub>50</sub> (mg·kg <sup>-1</sup> ) <sup>b</sup>	
Consensus method <sup>c</sup>	3337.72	1153.51
Hierarchical method <sup>d</sup>	2506.78	2421.17
FDA method <sup>e</sup>	6504.83	243.27
Nearest neighbor method <sup>f</sup>	2280.31	2605.88

<sup>a</sup> The data represent the mean ± SD of three independent experiments.

<sup>b</sup> Amount of chemical (mg·kg<sup>-1</sup> body weight) that causes 50% of rats to die after oral ingestion.

<sup>c</sup> The predicted toxicity is estimated by taking an average of the predicted toxicities from each of the above QSAR methodologies.

<sup>d</sup> The toxicity for a given query compound is estimated using the weighted average of the predictions from several different models. The different models are obtained by using Ward's method to divide the training set into a series of structurally similar clusters. A genetic algorithm-based technique is used to generate models for each cluster. The models are generated prior to runtime.

<sup>e</sup> The prediction for each test chemical is made using a new model that is fit to the chemicals that are most similar to the test compound. Each model is generated at runtime.

<sup>f</sup> The predicted toxicity is estimated by taking an average of the three chemicals in the training set that are most similar to the test chemical.

